

# Is attention truly all we need? An empirical study of asset pricing in pretrained RNN sparse and global attention models

Shanyan Lai<sup>1\*</sup>

<sup>1\*</sup>Department of Economics and Related Studies, University of York,  
Heslington, York, YO10 5DD, UK.

Corresponding author(s). E-mail(s): [shanyan.lai@york.ac.uk](mailto:shanyan.lai@york.ac.uk),  
[annieyanyan125@gmail.com](mailto:annieyanyan125@gmail.com);

## Abstract

This study investigates the pretrained RNN attention models with the mainstream attention mechanisms such as additive attention, Luong’s three attentions, global self-attention (Self\_att) and sliding window sparse attention (Sparse\_att) for the empirical asset pricing research on top 420 large-cap US stocks. This is the first paper on the large-scale state-of-the-art (SOTA) attention mechanisms applied in the asset pricing context. They overcome the limitations of the traditional machine learning (ML) based asset pricing, such as mis-capturing the temporal dependency and short memory. Moreover, the enforced causal masks in the attention mechanisms address the future data leaking issue ignored by the more advanced attention-based models, such as the classic Transformer. The proposed attention models also consider the temporal sparsity characteristic of asset pricing data and mitigate potential overfitting issues by deploying the simplified model structures. This provides some insights for future empirical economic research. All models are examined in three periods, which cover pre-COVID-19 (mild uptrend), COVID-19 (steep uptrend with a large drawdown) and one year post-COVID-19 (sideways movement with high fluctuations), for testing the stability of these models under extreme market conditions. The study finds that in value-weighted portfolio back testing, Model Self\_att and Model Sparse\_att exhibit great capabilities in deriving the absolute returns and hedging downside risks, while they achieve an annualized Sortino ratio of 2.0 and 1.80 respectively in the period with COVID-19. And Model Sparse\_att performs more stably than Model Self\_att from the perspective of absolute portfolio returns with respect to the size of stocks’ market capitalization.

**Keywords:** RNN, attention mechanisms, asset pricing, factor models

## 1 Introduction

Lai [1] proposes the dynamic MLP models for reducing the dimension of 'factor zoo' [2] of the asset pricing factor model, which is inspired by the work of Gu et al. [3] (GKX2020) and Coqueret and Guida [4]. It employs a dynamic structural algorithm from Coqueret and Guida [4] on MLP models to generate a hidden layer structure for the proposed MLP models as a substitute for the fixed pyramidal MLP structure of GKX2020's MLP models. It also substitutes the transformed firm characteristic factors of GKX2020's work to the firm characteristic-sorted portfolio [5] factors as the input factors to increase the interpretability of the asset pricing factor model in machine learning (ML) methods. The out-of-sample (OOS) fitness of the proposed MLP model with 2 hidden layers significantly outperforms traditional statistical models and GKX2020's benchmarks in both the pre-pandemic period (1911) and pandemic period (2112). Moreover, it shows a great advantage in mitigating downside risks caused by extreme market fluctuations (e.g. COVID-19).

However, as discussed in Zhou and Wang [6], although early ML models present excellent capabilities in modelling non-linear structure in financial and economic time-series data, fewer authors notice that early ML models, such as MLP, random forest(RF), Support Vector Machine (SVM) and MLP autoencoder, are not originally designed for time-series data. They only assume that these models naturally understand the temporal dependency of the data, and the data follows the independent and identically distributed (i.i.d.), or attempt to force a temporal sequence via the extending or rolling window methods. However, extending or rolling window methods face a dilemma for such tasks: the larger window size has a lower capability to capture the temporal dependency since the temporal dependency inside the window cannot be recognised; the smaller window size has a higher capability to detect the temporal dependency, but increases the possibility of model overfitting due to its small training data size. Therefore, exploring alternative ML structures originally developed the temporal mechanism, such as the recurrent neural networks (RNN, LSTM, GRU), which releases the aforementioned assumption, could be meaningful for ML-based asset pricing research. Moreover, GKX2020's work extends the dimension of the factors through the Kronecker product of firm characteristics and the macroeconomic indicators for the cross-sectional study and enlarges the data size for ML models. This does not assist the 'factor zoo' issue but brings their research into serious doubt of pure data-mining exercises. Thus, improving the model interpretability in ML asset pricing research could be another meaningful exercise, even if the study in Chapter 1 has already highly reduced the dimension of factors. Additionally, apart from capturing the sequential information of time-series data, how far the model can capture the historical information away from the current time step of a time-series, which is known as the 'memory' of the model, is an alternative crucial aspect for financial and

economic time-series modelling. Thus, searching for mechanisms that can enlarge the memory of recurrent neural network models which could further improve the model performance without sacrificing the model simplicity for computational efficiency and model interpretability, can be meaningful as well. Furthermore, GKX2020 as the seminal work for the ML-based asset pricing, focuses on the predictability of the ML models instead of evaluating pricing mechanisms, for example, how to explain the pricing error  $\alpha$ , how to improve the OOS model fitness ( $R^2$ ), and how to ensure the consistency of pricing performance over time.

Building on the findings of Lai [1], this study introduces a pre-trained recurrent neural network (RNN) architecture enhanced with self-attention mechanisms for addressing the aforementioned problems. Specifically, this study proposed two pre-trained RNN attention models: the RNN global self-attention model (self\_att) and the RNN sliding window sparse attention model (sparse\_att). In the proposed structures, the MLP autoencoder is deployed as the pre-trained method for the factors' dimensional reduction task, which further compresses the input factors' dimension into 70% of the original factors' dimension and reconstructs the missing values of the original factors. This process is also known as feature abstraction or feature engineering in ML methods. The RNN structure [7] was developed to overcome the limitation of the MLP [8] models, which the MLP models cannot handle sequential data naturally, especially time-series data. Unlike feedforward network models such as MLP, RNNs develop a hidden state that is updated recurrently over time, which enables the network to process input sequences. Concretely, the hidden state at each time step is calculated based on both the information of the current time step and the previous hidden state. This allows RNNs to learn patterns across time. Nevertheless, the vanilla RNN model does not overcome the issues of gradient vanishing and explosion existing in feedforward network models, especially when it is estimated by the stochastic gradient descent method (SGD). Although such issues can be mitigated through multiple approaches, such as adding L1 regularization to the loss function or using the Adam optimizer with the SGD method, the gradient vanishing issue remains more challenging. It causes the short 'memory' of the model, which prevents the RNN model from effectively capturing long-term dependencies in the sequence.

Fortunately, LSTM [9] and GRU [10] as RNN variation models extend the memory of the classic RNN to a degree in a general perspective. However, since the temporal sparsity characteristic of the asset pricing data, which presents as a smaller data size with longer time dependency, the LSTM model and the GRU model's high parameterization nature may cause overfitting. Thus, the most prevailing attention mechanism, the dot product based self-attention mechanism [11] and its sparse version, the sliding window attention mechanism [12], which are designed for the most prevalent large language models (LLM), Transformers, could be a great substitute of LSTM and GRU for balancing the trade-off between the model parameterization complexity and longer-term temporal dependency capturing. This study also further investigates whether the classic attention mechanisms generally improve the asset pricing and factor investing performance by constructing the pre-trained RNN additive attention

model (Batt), the pre-trained RNN Luong’s general attention model (LG), the pre-trained RNN Luong’s dot product attention model (LD) and the pre-trained RNN Luong’s concatenation attention model (LC) as benchmark models. These attention mechanisms were originally developed for natural language processing (NLP) tasks, and some of them are examined in the asset pricing tasks such as Zhou and Wang [6], Kelly et al. [13]. The proposed models and benchmark models are examined and back tested in three periods to show their capabilities of handling the extreme market conditions, which cover the period of pre-COVID-19 (1911), the COVID-19 (2112) and one year post-COVID-19 (2212). To the best of my knowledge, this is the first study for a large-scale investigation focusing on attention mechanisms in the asset pricing context. The MLP-pretrained RNN global self-attention model and RNN sliding-window sparse attention model, as innovative time-series tailored architectures, are introduced here and examined for the first time in asset pricing research.

Therefore, the contributions of this study can be considered from five angles:

- Employed MLP autoencoder as the pre-trained method for handling the missing values in firm characteristic-sorted portfolio factors and the dimensional reduction method for improving computational efficiency and mitigating the potential model overfitting issue.
- Examined the RNN structures on firm characteristic-sorted portfolio pretrained factors as a solution for capturing the temporal dependency of the data.
- Proposed two RNN attention variation models for asset pricing and factor investing contexts, the pre-trained RNN global self-attention model and the pre-trained RNN sliding window sparse attention model.
- Investigated the necessity of RNN classic attention models, such as additive attention and Luong’s three attention models, in the context of asset pricing and factor investing.
- Tested models’ capabilities of handling the extreme market conditions during the period of pre-COVID-19 (1911), the COVID-19 (2112) and one year post-COVID-19 (2212).
- Enforced the causal mask on the attention mechanism for time-series to prevent the future information leaking problem, which is ignored by recent attention-based research on financial and economic time-series data.

The study is organized into 6 sections. Section 2 introduces the related work of this research, while Section 3 describes the data employed in this study. Section 4 depicts the models deployed for this research. Section 5 shows the methods for evaluating the model performance and the back-testing performance, as well as an analysis of the empirical results. The conclusion and further discussion are presented in Section 6.

## 2 Related work

Traditionally, researchers focus on the linear and non-linear statistical function forms for asset pricing factor models. The most well-known model in the early stage of



asset pricing research is Fama and French [14], which firstly utilizes the market risk premium, firm characteristic-sorted portfolios of market capitalization size and book-to-market value size as factors for pricing dual-sorted US stock portfolios. It employs the significance level of the linear model intercept  $\alpha$  and the out-of-sample (OOS) fitness  $R^2$  as indicators to prove whether the portfolio returns are successfully being explained by the selected factors, which satisfies the market no-arbitrage assumption. This brings the enthusiasm for the later researchers to explore more innovative factors for a better explanation of stock excess returns. The works of Carhart [15], Fama and French [16], Hou et al. [17] can be the most representative examples. However, the increasing number of factors being explored and these factors are developed into a 'factor zoo'[18], which brings the dimensional disaster for the traditional statistical function form. Equation (1) depicts the linear form of the empirical asset pricing factor model, where  $r_{i,t+1}$  is the stock excess return at time  $t+1$ .  $\alpha_i$  is the intercept of the linear model, it is also known as anomaly, pricing error, abnormal return and return from mispricing in the context of asset pricing.  $\beta_i$  is the factor loading or factor exposure. If the no-arbitrage assumption stands,  $\alpha_i$  should approach zero, which means the risk premium can be fully explained by factor exposure  $\beta_i$ .

$$r_{i,t+1} = \alpha_i + \beta_i^\top f_{t+1} + \varepsilon_{i,t+1} \quad (1)$$

Fortunately, the burgeoning of AI algorithms provides some great solutions for the dimensional disaster challenge of asset pricing research. The seminal work of this domain is Gu et al. [3]'s 'empirical asset pricing in machine learning'. It examines the majority of traditional ML models, such as MLP, SVM, RF and gradient boosting, on 94 firm characteristics and 8 macroeconomic indicators cross-sectionally from the US stock market, and it proves that MLP with 3 hidden layers outperforms all alternative models on large-dimension factors. This work is followed by Wang [19], which tests Gu et al. [3]'s models on cryptocurrency pricing. It finds that the MLP with 3 hidden layers is the best model in the cryptocurrency market as well. Later, Gu et al. [20] proposed a structure based on two MLP autoencoders for asset pricing tasks. One for generating  $\beta$ s for factors and the other for factors' dimensional reduction. By dot producting the output of the two MLP autoencoders, it achieves a better performance than Gu et al. [3]'s best-performing model. Equation (2) shows the additive form, and Equation (3) shows the general form of the asset pricing factor model. Both of Gu et al. [3, 20] agree that in ML-based empirical asset pricing research, the concentration is on exploring the function form of  $g(f_{i,t}; \theta)$ . That is the foundation of later research in this direction.

$$r_{i,t+1} = \mathbb{E}_t[r_{i,t+1}] + \varepsilon_{i,t+1} \quad (2)$$

$$r_{i,t+1} = g(f_{i,t}; \theta) + \varepsilon_{i,t+1} \quad (3)$$

Avramov et al. [21] conduct a comparative study on the MLP model with three hidden layers of Gu et al. [3], the generative adversarial neural network model with RNN cores of Chen et al. [22], the instrumental PCA model of Kelly et al. [23]

and the conditional autoencoder extension of Gu et al. [20] in the US stock market from a portfolio strategy-wise perspective. It imposes economic constraints in these models and improves the economic interpretability of the traditional ML models for asset pricing research. They prove that the trading strategies based on traditional ML methods have a great preference for hedging downside risks during the market crisis, especially in value-weighted portfolio configurations. They also confirm that ML trading signals in favour of long-only positions and achieve considerable profit compared with alternative strategies such as long-short spread and short-only positions. It suggests that the small-cap stocks and distressed stocks should be excluded for a better representation of the market, while the profitability of the ML-based strategy can be improved by focusing only on the long-only strategy. Bagnara [24] conduct a comprehensive and critical survey of recent developments at asset pricing in machine learning (ML), with a particular focus on addressing the long-standing “factor zoo” problem. The review mainly investigates the classic ML methods and classifies the literature into five methodological categories—regularization, dimension reduction, regression trees and random forests, neural networks, and comparative analyses—applied within two main frameworks: empirical factor modelling with return prediction and stochastic discount factor (SDF) estimation. Its comparative studies find that boosted trees and neural networks outperform linear benchmarks in predictive accuracy. It proposes the persistent challenges, including limited economic interpretability of the ML models, risk of data-snooping, and weak integration with causal inference, and calls for hybrid approaches combining economic theory, robust time-series validation, and evaluation based on economically meaningful metrics such as portfolio-wise performance. Moreover, it agrees with the conclusion from Avramov et al. [21] that the economic value of ML-based strategies often lies less in boosting unconditional average returns, but rather in their ability to hedge downside risk and preserve capital during downturns or crisis periods.

Although traditional ML-based asset pricing literature provides much evidence that early-stage ML models have advantages in improving prediction accuracy and mitigating market downside fluctuation risks, they face the problems of the compliance of ML models and the asset pricing context. For example, MLP, SVM and RF are not designed for sequential or time-series data originally, but early literature imposes the assumption of sequence recognition when they are applied to sequential data. This may affect the prediction accuracy or increase the probability of model misspecification and overfitting, even if extending or rolling window methods are deployed. Thankfully, later literature with the second generation of ML models, such as the RNN model and its variations, solves the problem due to the sequential nature of these models. Different from empirical asset pricing, Chen et al. [22] applies a generative adversarial network (GAN), which is proposed by Goodfellow et al. [25], for the stochastic discount factor (SDF) asset pricing approach. It adopts the feedforward MLP for the dimensional reduction of the firm characteristics cross-sectionally, and LSTM to generate the economic states for large-scale macroeconomic indicators. Henceforth, generating a candidate SDF through the generator of GAN, and evaluating it via the discriminator of GAN to impose the minimum pricing error

$\alpha$  converging to zero to satisfy the no-arbitrage assumption. Namely, it configures the no-arbitrage as the training goal of the entire model. It shows the superiority of traditional ML models and proves that the LSTM macroeconomic states promote the model performance significantly. Their work fantastically addresses the suitability for time-series data through the LSTM model and statistically defends the no-arbitrage hypothesis. However, if the market exists arbitrage opportunities, which is possibly caused by price limits or liquidity fractions, even the most powerful GAN can only fit an approximate SDF rather than the true pricing kernel. Moreover, although the authors attempt to interpret factor importance, it is difficult to provide clear economic meanings comparable to traditional factors. Additionally, the model may face issues as mode collapse and non-convergence, which cause training instability, while statistically minimizing the  $\alpha$  may raise the suspicion of data snooping. In this sense, our proposed models on the RNN foundations and the empirical factor settings are simpler and more interpretable, which respects the real market conditions.

However, the application of RNNs and attention mechanisms to asset pricing remains at a very early and cutting-edge stage, and the extant literature remains relatively sparse. The most relevant literature of this study is Zhou and Wang [6], which is developed from the work of Gu et al. [20]. It keeps the MLP structure for calculating the factor loadings, but alters the MLP autoencoder to the RNN additive attention structures for factor dimensional reduction. By dot producting the output factor loadings from the MLP structure and the abstracted factors from the RNN additive attention structures, the estimated stock excess returns can be computed. It resolves the temporal dependency capturing issue through the exchange models of RNN, LSTM and GRU, while adopting the additive attention mechanism for extending the memory for long-term temporal dependency of the asset pricing data. Its LSTM additive attention model with the abstracted six factors outperforms all benchmark models, including Gu et al. [20] and Kelly et al. [23]. Nonetheless, it does not explain how they decide the dimension of abstracted factors, nor how to explain these alternative factors, which covers their models with the 'black-box' shadows. Furthermore, the additive attention mechanism extends the memory for capturing the longer-term temporal dependency of the data, which potentially improves the prediction accuracy, but the limited data size may cause overfitting due to the complication of the model with high parameter numbers. Moreover, as the model applies the attention mechanism to the overall hidden states of RNN outputs, which have temporal properties, it should embed causal masks to prevent future information leaking. Otherwise, it introduces the look-ahead bias, which may cause spurious performance, loss of economic interpretability, non-tradable strategy and data snooping issues. However, it is a common issue in recent attention-based asset pricing research, including the work of Kelly et al. [13], Ma et al. [26], Zhang [27] and Cong et al. [28]. Our attention models notice this problem and enforce a causal mask individually to satisfy the single-direction characteristic of the time-series data.

Interestingly, recent works concentrate on the application of prevailing large language models (LLMs), such as Transformers, which contain multiple attention mechanisms,

instead of simplified models that focus on attention mechanisms themselves. For example, Cong et al. [28] implements a comparative study of ML models with the temporal dependency capture nature, such as RNN, single or bi-directional LSTM, RNN with additive and classic Transformer, for empirical asset pricing on large-scale US stocks. In their study, LSTM achieves the best OOS fitness, but GRU derives the highest annulized Sharpe ratio from the long-short portfolio. Zhang [27] conducts a similar comparative study to Cong et al. [28]. It compares MLP and MLP residual, Convolutional Neural Network (CNN) and CNN residual, RNNs, RNN additive attention, classic Transformer model and traditional ML models. It finds that the RNN additive attention model slightly outperforms the classic Transformer model, achieving the highest OOS  $R^2$ . Ma et al. [26] proposes a CNN multi-head self-attention-based encoder-only Transformer model for Chinese stock pricing and volatility forecasting from January 2000 to December 2019. It uses 72 firm characteristics and 8 macroeconomic indicators as the pricing factors and volatility forecasting results for calculating asset allocation weights. The Transformer model with three encoder blocks outperforms all alternative variations and traditional ML benchmarks. It proves that the Transformer model with the multi-head self-attention mechanism performs well in return forecasting and even better in volatility forecasting. Although these works inspire later researchers with the ML function form for asset pricing, the largest problem of these works is neglecting the single-direction characteristic of the time-series data, since none of them imposes the causal mask to prevent the future information leaking, even if they are mitigated by sequential methods, such as the rolling window and the extending window. Additionally, most of these works employ the data ended in the year of 2016, which excludes the extreme market conditions caused by the COVID-19 pandemic. Namely, they did not examine the model performance during the market turbulence to show the stability of the models they applied. Instead, this study employs three periods, which cover the stages of pre-pandemic, pandemic and a year post-pandemic, and investigates how the typical RNN-based attention models react to the COVID-19 pandemic effect. Furthermore, most of these works deploy firm characteristics and macroeconomic indicators directly as the input factors, which raises the suspicion of data snooping or data mining as well. In this study, the firm characteristics-sorted portfolios are applied as the original input factors, which cross-sectionally consider the information that covers the entire market and improve the economic explainability of the model.

Some of the asset pricing literature based on attention mechanisms appears to circumvent the future data leaking issue, as they apply it cross-sectionally rather than temporally. For example, Kelly et al. [13] cross-sectionally applies an encoder-only Transformer model with Luong’s general (bilinear form) attention mechanism for generating the best SDF at each time  $t$ , which derives the highest OOS Sharpe ratio. They examine their model on large-scale US stocks and 132 normalized firm characteristics as factors, while deploying a short rolling training window of 60 observations. Their work covers the entire period of the COVID-19 pandemic. And their model outperforms the MLPs and linear benchmark models. Nevertheless, they simply substitute the missing values in the firm characteristics with zero, but ignore

the input factors’ data quality. For LLMs, low data quality increases the probability of model hallucination, which introduces untruthful similarity between different firm characteristics and leads to incorrect predictions. Moreover, they generate the SDF at each time  $t$ , and combine it into a time-series-like sequence, but it neglects the temporal dependency to some extent. Still, the limited data size with a highly parameterized model structure increases the risk of model overfitting and lowers the model’s economic interpretability. The MLP autoencoder pre-trained method of this study is employed for handling the missing values in the input factors and reduces the input dimension to moderate model overfitting issues, which may also assist their method of asset pricing research. The simplified model structure in this study, with only an RNN and one attention layer, and the abstracted factors may conquer the general problems that exist in advanced ML-based asset pricing research. Similarly, Chatigny et al. [29] proposes an N-BEATS style architecture augmented with a linear self-attention mechanism, which cross-sectionally evaluates the importances of firm characteristics and macroeconomic variables. The model directly estimates the SDF by minimizing squared Euler equation errors, and reports remarkably strong out-of-sample performance with annualized Sharpe ratios exceeding 2.8 at the market level, and above 1.0 even after excluding the smallest stocks or restricting the stocks to the Russell 3000 constituents. Their linear self-attention improves economic interpretability by highlighting relevant macroeconomic and firm-level features during different market conditions (e.g., the 2008 crisis). This is an innovative work, but it still faces issues as it practically neglects the transaction costs for short-selling positions, market impact, or leverage constraints, which reduces the implementability in real-world trading. Additionally, although the missing firm characteristics are imputed with cross-sectional medians, which is a typical method commonly applied in the industry, it could induce systematic biases if the missing values are manipulated. It is also worth noting that their attention weights capture the statistical relevance of factors at each time point rather than structural causality and temporal dependencies. Thus, their high Sharpe ratio should be carefully confirmed the robustness, non-overfitting and non-data-snooping suspicion.

### 3 Data description

The proposed models and benchmarks employ sorted portfolio returns as observable factors, which are reconstructed by Andrew Y.; Zimmermann [5], to estimate individual stock returns. The 182 factors from Andrew Y.; Zimmermann [5], which excludes the factor with missing values larger than 40% for maintaining a reasonable data quality, are selected as the original input in this study. The stocks are selected from the US NASDAQ and NYSE, which are derived from Wharton Research Data Services (WRDS). 420 large-cap US stocks are selected from the top 15% of stocks ranked by market capitalization (MC), which covers 85% of total market capitalization for these two markets. They satisfy the conditions of no missing value in the testing period and less than 50% of missing values during the training period. This is

due to the consideration of ‘going concern’ in the real-market practice and data representability. Thus, this stock selection criterion, ‘too-big-to-fail’ and the assumption of ‘going concern’, is more realistic for practitioners since it protects the investors from systematic risks such as companies being delisted unexpectedly due to insolvency (e.g. Lehman Brothers). The selected 420 stocks finally cover approximately 21.38% of the overall market capitalization. Despite the proposed models deploying the MLP autoencoder as the pretrained method for dimensional reduction and information subtraction, excessive missing values can hinder model performance by reducing the effective information available for representation learning and increasing the risk of biased imputations, especially for models with attention mechanisms. The attention mechanisms may concentrate on unreliable or non-informative time steps, weakening local or global feature extractions. The biased imputations pose a risk, particularly in deep learning-based forecasting. If it is not properly constrained, it can introduce hallucinated inputs—values generated from prior correlations rather than observable causality, thus distorting both training and evaluation. In addition, the risk-free rate for constructing the excess stock returns and evaluating the Sharpe ratio and Sortino ratio is derived from the Kenneth R. French Data Library<sup>1</sup>.

The entire monthly data covers from January 1957 to December 2022. The separation of the training period, validation period and testing period is listed in Table 1. This study adopts the rolling window method instead of the prevailing extending window method in previous literature such as Gu et al. [3]. The validation window size is approximately 20% of the training size.

Name	Start date	End date	Observation No.
In-sample total	1/1957	12/2012	672
Testing (OOS) for ‘1911’	1/2013	11/2019	83
Testing (OOS) for ‘2112’	1/2013	12/2021	108
Testing (OOS) for ‘2212’	1/2013	12/2022	120

**Table 1:** Data splits for in-sample and out-of-sample data. ‘1911’ means the testing period ends before the pandemic happened, ‘2112’ means the testing period contains the pandemic period and ‘2212’ means the testing period contains not only the pandemic period but also one year after the pandemic.

## 4 Models

The pre-trained recurrent neural network (RNN) attention models employ the MLP autoencoder as the pertaining method for the dimensional reduction of the original input factors, which is the firm characteristic-sorted portfolios provided by Andrew Y.; Zimmermann [5], and handling the missing values. The pretrained factors (abstracted features or factors) then feed into the main models shown in Figure 2.

<sup>1</sup>[https://mba.tuck.dartmouth.edu/pages/faculty/ken.french/data\\_library.html](https://mba.tuck.dartmouth.edu/pages/faculty/ken.french/data_library.html)

The main models are organized by an RNN fundamental structure with an attention layer, which are introduced in Section 4.2 to Section 4.4. Figure 1 shows the entire workflow of the pretrained RNN attention models. This study investigates the RNN models with the additive attention mechanism [30], Luong attention mechanisms [31], global self-attention mechanism [11] and the sliding window sparse attention mechanism [12], and compares them with the vanilla RNN model and its variations: long short-term memory (LSTM) neural networks and gated recurrent unit (GRU) neural network. Among these RNN attention models, the RNN sliding window sparse attention model and the RNN self-attention model are the proposed RNN attention models. The RNN sliding window sparse attention model abstracts the sliding window sparse attention mechanism from the Longformer model [12], which is introduced in Section 4.3.4, while the RNN self-attention model abstracts the self-attention mechanism from the classic Transformer model [11], which is introduced in Section 4.3.3. Since the sliding window sparse attention belongs the category of self-attention, thus, in this study, the classic self-attention mechanism from [11] is denoted as 'global self-attention mechanism' for preventing any confusion.

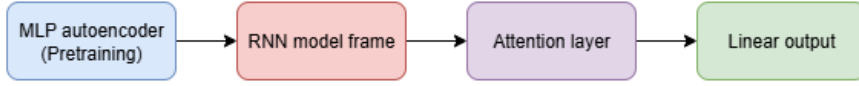


**Fig. 1:** The workflow diagram of the RNN attention models.

Figure 2 is the workflow diagram of the main models which assemble a two-hidden-layer vanilla RNN frame with an attention layer. An attention layer contains one attention mechanism, for example, the additive attention mechanism or one of Luong’s attention mechanisms. The left part of Figure 2 shows the main workflow of the RNN attention models. The input  $X$ , which is the pricing factors in this case, goes through the RNN hidden layers and the sliding window sparse attention layer, then derives the output  $\hat{y}$ . The loss function  $L$  measures the difference between the output derived from the RNN attention structure and the label  $y$ , which is the stock excess return series in this case.  $W$  is the learnable parameter matrix recurrently calculated according to the timeline. The right part exhibits the unfolded 3-dimensional structure of the RNN attention models, where the RNN frame has two pyramidal hidden layers:  $h^{(1)}$  and  $h^{(2)}$ . The first hidden layer and the second layer configure 64 and 32 neurons respectively. From the second dimension scope, the RNN structure collects the current and the one-step previous information and passes them to the next time step as introduced in Section 4.2. From the third dimension angle of the figure, each time step has a pyramidal MLP network, which achieves the goal of reducing the feature’s dimension. Additionally, the attention layer estimates and distributes the attention weights to each time step to depict the relevance of any two time steps in a pre-defined sight range. The attention output  $z_t$  is used for computing the estimated  $\hat{y}$  with a linear connection.



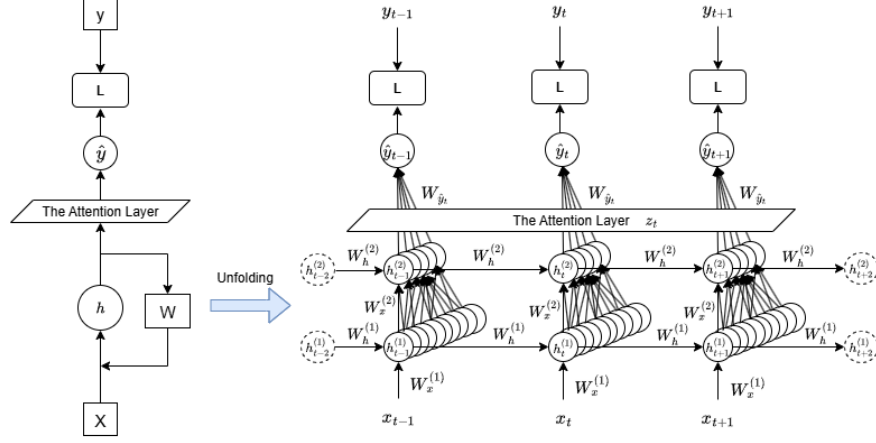


**Fig. 2:** The workflow diagram of the RNN attention models. In this figure,  $W_h^{(1)}$ ,  $W_h^{(2)}$ ,  $W_x^{(1)}$  and  $W_x^{(2)}$  are learnable parameter matrices for each layer,  $X$  and  $y$  are pretrained input and labels respectively.  $h$  indicates the hidden layers of the RNN structure,  $\hat{y}$  is the output derived from the attention layer after linear transformation, and  $L$  represents the loss function. The 'Attention layer' is the attention layer that contains an attention mechanism (e.g. additive attention mechanism or one of Luong's attention mechanisms). The left side of the figure is the main workflow of the RNN attention models, and the right side is the 3-Dimension timeline-based unfolded workflow diagram. The circles indicate the nodes of each hidden layer. Each node is fully connected to all nodes in the next layer.

#### 4.1 MLP autoencoder for perturbing

The MLP autoencoder is commonly used for feature engineering in the machine learning and financial time-series forecasting context, especially for dimensional reduction and data denoising purposes [32–36]. This study deploys the MLP autoencoder as a pre-training method for input factors' dimensional reduction and missing value filling. Figure 3 shows the MLP autoencoder module deployed for this study. The MLP autoencoder encompasses an input layer, an output layer (reconstructed layer in this case) and a latent layer (latent space or bottleneck layer) in between. The layer with green nodes is the input layer, and the one with red nodes indicates the reconstructed layer. The process from the input layer to the latent layer is named 'encoding', and from the latent layer to the reconstructed (output) layer is named 'decoding' in an autoencoder frame. The original input factors are denoted as  $f$ ,  $f \in \mathbb{R}^n$  and the reconstructed factors are recognized as  $\hat{f}$ ,  $\hat{f} \in \mathbb{R}^n$ . Through an MSE loss function  $L$ , the reconstructed factors can be trained to closely approach the actual input factors. The layer in between with blue nodes is the latent layer, where it subtracts the new factor with a lower dimension. The parameters which lead to the minimum MSE of the loss function are used to generate new factors. The new factors are denoted as  $x$ ,



$x \in \mathbb{R}^m, m < n$ . Therefore, the encoding process can be mathematically presented as:

$$\mathbf{X} = g(\mathbf{W}_{\text{en}}\mathbf{F} + \mathbf{b}_{\text{en}}) \quad (4)$$

where  $\mathbf{F} = [\mathbf{f}_1, \mathbf{f}_2, \dots, \mathbf{f}_n] \in \mathbb{R}^{n \times T}$  is the original input factor matrix,  $T$  is the time length, while  $\mathbf{X} = [\mathbf{x}_1, \mathbf{x}_2, \dots, \mathbf{x}_m] \in \mathbb{R}^{m \times T}$  is the latent factor matrix.  $\mathbf{W}_{\text{en}} \in \mathbb{R}^{m \times n}$  and  $\mathbf{b}_{\text{en}} \in \mathbb{R}^{m \times 1}$  are the weight matrix and bias of the encoder respectively.  $g(\cdot)$  is the Rectified Linear Unit (ReLU) activation function  $\text{ReLU}(x) = \max(0, x)$ . The function of the encoding is to lower the dimension of the original input factors.

The function of the decoding is opposite to the function of the encoding. It attempts to reconstruct the original input factors. It utilizes a loss function to measure the accuracy of the reconstructed factors, and it can be presented as:

$$\hat{\mathbf{F}} = g(\mathbf{W}_{\text{de}}\mathbf{X} + \mathbf{b}_{\text{de}}) \quad (5)$$

where  $\mathbf{W}_{\text{de}} \in \mathbb{R}^{n \times m}$  and  $\mathbf{b}_{\text{de}} \in \mathbb{R}^{n \times 1}$  are the decoder weight matrix and bias, respectively.  $\hat{\mathbf{F}} = [\hat{\mathbf{f}}_1, \hat{\mathbf{f}}_2, \dots, \hat{\mathbf{f}}_T] \in \mathbb{R}^{n \times T}$  are the estimated original factors. Considering the balance of the information effectiveness and the noise level of the generated latent factors, the neuron number is configured 70% of the original input.

The mean square error (MSE) function is selected as the loss function for estimating the accuracy of factor reconstruction, which is shown in Equation (6). Stochastic gradient descent (SGD) algorithm with Adaptive moment estimation (Adam) optimizer is employed for the estimation and early-stopping method are applied for improving computational efficiency and preventing model overfitting caused by training process. They are presented in the Appendix.

$$\mathcal{L}_{\text{recon}} = \frac{1}{T} \left\| \mathbf{F} - \hat{\mathbf{F}} \right\|_F^2 \quad (6)$$

## 4.2 Recurrent Neural Networks

The fundamental structure of the proposed model is the RNN structure, which is shown in the left part of Figure 2. The workflow chart without the sparse attention layer is the naive RNN structure. A fundamental RNN structure includes an input layer, an output layer and a single or multiple hidden layer. In this study, for a better capture of factor patterns, two hidden layers with a pyramid neuron structure are employed, specifically, the first hidden layer with 64 neurons and the second hidden layer with 32 neurons. The mathematical presentation of the multilayer RNN model is presented in Equation (7) to Equation (11), where  $\mathbf{h}_t^{(1)}$  and  $\mathbf{h}_t^{(2)}$  mean the output of the first hidden layer and the second hidden layer at time  $t$ .  $\mathbf{h}_{t-1}^{(1)}$  and  $\mathbf{h}_{t-1}^{(2)}$  are the output of hidden layers at time  $t-1$ , while  $\mathbf{x}_t$  is the abstracted factors from pre-training module.  $\mathbf{W}_h^{(1)}$ ,  $\mathbf{W}_h^{(2)}$ ,  $\mathbf{W}_x^{(1)}$  and  $\mathbf{W}_x^{(2)}$  are the estimated parameter matrices of the previous hidden states and current inputs respectively.  $\mathbf{b}_{rnn}^{(1)}$  and  $\mathbf{b}_{rnn}^{(2)}$  are the bias of each hidden layers.

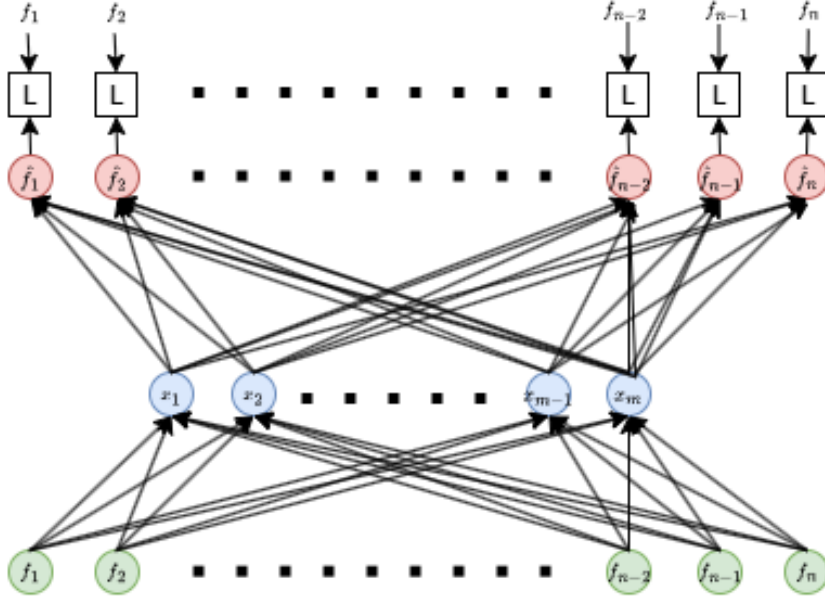


**Fig. 3:** MLP autoencoder as the pre-training module. In this figure,  $f_1, f_2$  to  $f_n, n \in \mathbb{Z}^+$  are denoted as original factors.  $L$  is the loss function, MSE in this case.  $\hat{f}_1, \hat{f}_2$  to  $\hat{f}_n, n \in \mathbb{Z}^+$  are the reconstructed factors. The bottom layer with green nodes is the input layer, while the top layer with red nodes is the reconstructed layer. The layer in between with blue nodes named latent space of the autoencoder, which generates the new factors with a lower dimension, where  $x_1$  to  $x_m, m \in \mathbb{Z}^+$  denoted as new factors.

$$\mathbf{h}_t^{(1)} = \phi \left( \mathbf{W}_h^{(1)} \mathbf{h}_{t-1}^{(1)} + \mathbf{W}_x^{(1)} \mathbf{x}_t + \mathbf{b}_{rnn}^{(1)} \right), \quad \mathbf{h}_t^{(1)} \in \mathbb{R}^{64} \quad (7)$$

$$\mathbf{h}_t^{(2)} = \phi \left( \mathbf{W}_h^{(2)} \mathbf{h}_{t-1}^{(2)} + \mathbf{W}_x^{(2)} \mathbf{h}_t^{(1)} + \mathbf{b}_{rnn}^{(2)} \right), \quad \mathbf{h}_t^{(2)} \in \mathbb{R}^{32} \quad (8)$$

And  $\phi(\cdot)$  is the hyperbolic tangent ( $\tanh$ ) activation function, can be written as:

$$\tanh(z) = \frac{e^z - e^{-z}}{e^z + e^{-z}} \quad (9)$$

if,

$$z = \mathbf{W}_h^{(1)} \mathbf{h}_{t-1}^{(1)} + \mathbf{W}_x^{(1)} \mathbf{x}_t + \mathbf{b}_{rnn}^{(1)} \quad (10)$$

or,

$$z = \mathbf{W}_h^{(2)} \mathbf{h}_{t-1}^{(2)} + \mathbf{W}_x^{(2)} \mathbf{h}_t^{(1)} + \mathbf{b}_{rnn}^{(2)} \quad (11)$$

### 4.3 Attention mechanisms for attention layer

The attention mechanism is a powerful neural network component that enables models to dynamically focus on the most relevant parts of a sequence when making predictions. It was originally developed for the context of natural language processing (NLP), such as missing text prediction and machine translation. It employs a function to compute the attention scores to measure the relevance level between any two parts of a textual sequence, and applies the softmax function to normalize the attention scores to attention weights to measure the importance of each word. Thus, the attention mechanism can improve the textual prediction accuracy through the indicator shows the importance of a certain word.

The earliest attention mechanism is the additive attention mechanism from Bahdanau et al. [30]. Gradually, researchers developed different function forms for the attention mechanism. Luong’s three-form attention mechanism [31] is one of the most significant attention mechanisms. However, the attention mechanisms cannot directly apply to time-series data such as factors and stock returns, since the textual data is sometimes bidirectional. For instance, the missing word prediction could depend not only on the previous words but also on the words behind the missing space. However, the time-series forecasting only relies on historical data, which implies that bidirectional forecasting may cause the future data leak issue. Therefore, a compulsory causal mask which can cover future data is crucial for time-series attention mechanism applications. For time-series attention mechanisms, the attention weights, which measure the relevance level of two time steps, are only computed between the current time step and the historical time steps, but the future time steps are covered by masks. And the attention weights are finally distributed back to the fundamental structure (e.g. RNN or LSTM) output to generate attention output, combining the information of the fundamental structure output and the importance of the information at each time step. The research on applications of attention mechanisms for finance and economics is still in the early stages. As an example, Kelly et al. [13] deploys Luong’s general attention mechanism to their Transformer model for the asset pricing research.

Attention mechanisms have three essential elements: query, key and value. Query and key are used for computing attention scores via a certain function form, while value is used for computing the attention output. The global self-attention mechanism [11] and sliding window attention mechanism [12] have explicit values since they have a specific function form for the element of ‘value’, but alternative attention mechanisms have hidden value equal to the historical output of the foundation neural network structure. The additive attention[30], which employs a feedforward network to compute alignment scores, is introduced in Section 4.3.1. The multiplicative (or general) attention[31], which uses linear forms to compute the similarity between queries and keys, is introduced in Section 4.3.2. Scaled dot-product attention [11, 31] further improves numerical stability and training efficiency by introducing a scaling factor, and it serves as the foundation of the most prevailing large language model named Transformer. This is introduced in Section 4.3.3 and Section 4.3.4.

#### 4.3.1 Additive attention mechanism

Bahdanau et al. [30]’s additive attention is the earliest attention mechanism originally designed for natural language processing (NLP) tasks such as machine translation. As a global attention mechanism, it measures the difference between any two time steps and distributes attention weights for every time step. It is suitable for capturing the most relevant information from context which could increase the prediction accuracy of the missing words within a sentence. However, this causes the future information leak if the attention mechanism is applied directly to the time series data without a causal mask. Let  $\mathbf{q}_t, \mathbf{k}_j \in \mathbb{R}^{d_{RNN}}$  be the query and key of at time step of  $t$  and  $j$ , and define:

$$\mathbf{q}_t = \mathbf{W}_q \mathbf{h}_t^{(2)}, \quad \mathbf{k}_j = \mathbf{W}_k \mathbf{h}_j^{(2)} \quad (12)$$

where  $\mathbf{W}_q, \mathbf{W}_k \in \mathbb{R}^{d_{RNN} \times d_{RNN}}$  are the learnable parameter matrices of  $\mathbf{h}_t^{(2)}, \mathbf{h}_j^{(2)} \in \mathbb{R}^{d_{RNN}}$ . Then the additive attention score for time  $t$  and  $j$ ,  $e_{t,j}$ , can be presented as:

$$e_{t,j} = \mathbf{v}^\top \tanh(\mathbf{q}_t + \mathbf{k}_j) \quad (13)$$

where  $\mathbf{v} \in \mathbb{R}^{d_{RNN}}$  is a learnable parameter vector. Considering the input is the time-series data, the compulsory causal mask should be applied to force time step  $j$  to be earlier than  $t$ . Thus, the attention score  $e_{t,j}$  with masks can be:

$$e_{t,j} = \begin{cases} \mathbf{v}^\top \tanh(\mathbf{q}_t + \mathbf{k}_j), & \text{if } j \leq t \\ -\infty, & \text{if } j > t \end{cases} \quad (14)$$

With the attention scores, the attention weights can be calculated via a softmax function,

$$\alpha_{t,j} = \frac{\exp(e_{t,j})}{\sum_{i=1}^t \exp(e_{t,i})} \quad (15)$$

Thus, the attention output  $\mathbf{z}_t \in \mathbb{R}^{d_{RNN}}$  is the summation of the attention weighted historical RNN output  $\mathbf{h}_j^{(2)}$ .

$$\mathbf{z}_t = \sum_{j=1}^t \alpha_{t,j} \mathbf{h}_j^{(2)} \quad (16)$$

#### 4.3.2 Luong’s attention mechanism

Luong’s attention is developed from the additive attention. Luong et al. [31] proposes three attention weights computation methods for boosting the computational efficiency and forecasting accuracy of Bahdanau et al. [30]’s additive attention. It employs the dot product, linear and concatenation for computing the attention weights respectively, which are defined as ’Luong dot-product (LD) attention’, ’Luong general (LG) attention’ and ’Luong concatenation (LC) attention’.

For Luong dot-product attention, the query  $\mathbf{q}_t$  and key  $\mathbf{k}_j$  is equal to the RNN output at time  $t$  and  $j$ , which shows in Equation (17)

$$\mathbf{q}_t^{LD} = \mathbf{h}_t^{(2)}, \quad \mathbf{k}_j^{LD} = \mathbf{h}_j^{(2)} \quad (17)$$

The Luong dot-product attention score  $e_{t,j}$  is the scaled dot product of query  $\mathbf{q}_t$  and key  $\mathbf{k}_j$ ,

$$e_{t,j}^{LD} = \frac{1}{\sqrt{d_{\text{RNN}}}} (\mathbf{q}_t^{LD})^\top \mathbf{k}_j^{LD} \quad (18)$$

$$= \frac{1}{\sqrt{d_{\text{RNN}}}} (\mathbf{h}_t^{(2)})^\top \mathbf{h}_j^{(2)} \quad (19)$$

The causal mask setting in this case is similar to alternative global attention mechanisms,

$$e_{t,j}^{LD} = \begin{cases} \frac{1}{\sqrt{d}} (\mathbf{q}_t^{LD})^\top \mathbf{k}_j^{LD}, & \text{if } j \leq t \\ -\infty, & \text{if } j > t \end{cases} \quad (20)$$

Thus, the attention weights and output for the Luong dot-product attention are:

$$\alpha_{t,j}^{LD} = \frac{\exp(e_{t,j}^{LD})}{\sum_{i=1}^t \exp(e_{t,i}^{LD})} \quad (21)$$

$$\mathbf{z}_t^{LD} = \sum_{j=1}^t \alpha_{t,j}^{LD} \mathbf{h}_j^{(2)} \quad (22)$$

For Luong's general attention mechanism, it distributes a learnable parameter matrix  $\mathbf{W} \in \mathbb{R}^{d_{\text{RNN}} \times d_{\text{RNN}}}$  to the key  $\mathbf{k}_j$  but keep the query  $\mathbf{q}_t$  identical to the one in Luong dot-product attention. It projects key to the query linearly by adding the parameter matrix  $\mathbf{W}$ . Equation (23) shows the query and key for Luong's general attention mechanism.

$$\mathbf{q}_t^{LG} = \mathbf{h}_t^{(2)}, \quad \mathbf{k}_j^{LG} = \mathbf{W} \mathbf{h}_j^{(2)} \quad (23)$$

Thus, the attention score of Luong's general attention can be:

$$e_{t,j}^{LG} = \frac{1}{\sqrt{d_{\text{RNN}}}} (\mathbf{q}_t^{LG})^\top \mathbf{W} \mathbf{k}_j^{LG} \quad (24)$$

Similarly, with the mask for the causality,

$$e_{t,j}^{LG} = \begin{cases} \frac{1}{\sqrt{d_{\text{RNN}}}} (\mathbf{q}_t^{LG})^\top \mathbf{W} \mathbf{k}_j^{LG}, & j \leq t \\ -\infty, & j > t \end{cases} \quad (25)$$

After the LG attention scores  $e_{t,j}^{\text{LG}}$  are computed, it can be used for computing the LG attention weights  $\alpha_{t,j}^{\text{LG}}$  and the attention output  $\mathbf{z}_t^{\text{LG}} \in \mathbb{R}^{d_{\text{RNN}}}$ :

$$\alpha_{t,j}^{\text{LG}} = \frac{\exp(e_{t,j}^{\text{LG}})}{\sum_{i=1}^t \exp(e_{t,i}^{\text{LG}})} \quad (26)$$

$$\mathbf{z}_t^{\text{LG}} = \sum_{j=1}^t \alpha_{t,j}^{\text{LG}} \mathbf{h}_j^{(2)} \quad (27)$$

For Luong's concatenation attention mechanism, the query  $\mathbf{q}_t^{\text{LC}}$  and key  $\mathbf{k}_j^{\text{LC}}$  have their own learnable parameter matrix which denoted as  $\mathbf{W}_q$  and  $\mathbf{W}_k$  respectively,  $\mathbf{W}_q, \mathbf{W}_k \in \mathbb{R}^{d_{\text{RNN}} \times d_{\text{RNN}}}$ . Concretely, the query and key can be presented as:

$$\mathbf{q}_t^{\text{LC}} = \mathbf{W}_q \mathbf{h}_t^{(2)}, \quad \mathbf{k}_j^{\text{LC}} = \mathbf{W}_k \mathbf{h}_j^{(2)} \quad (28)$$

Different from all alternative attention mechanisms, Luong's concatenation attention applies a hyperbolic tangent function on the concatenated query and key for calculating the attention scores. The Luong's concatenation attention score can be computed as:

$$e_{t,j}^{\text{LC}} = \mathbf{v}^\top \tanh([\mathbf{q}_t^{\text{LC}}; \mathbf{k}_j^{\text{LC}}]) \quad (29)$$

where  $\mathbf{v} \in \mathbb{R}^{2d_{\text{RNN}}}$  is the learnable parameter vector for calculating the concatenation attention scores. For time-series specific data, the attention score with causal mask can be extended as:

$$e_{t,j}^{\text{LC}} = \begin{cases} \mathbf{v}^\top \tanh([\mathbf{q}_t^{\text{LC}}; \mathbf{k}_j^{\text{LC}}]), & j \leq t \\ -\infty, & j > t \end{cases} \quad (30)$$

By following similar process of alternative attention mechanisms, the attention weights and attention outputs of Luong's concatenation attention can be written as:

$$\alpha_{t,j}^{\text{LC}} = \frac{\exp(e_{t,j}^{\text{LC}})}{\sum_{i=1}^t \exp(e_{t,i}^{\text{LC}})} \quad (31)$$

$$\mathbf{z}_t^{\text{LC}} = \sum_{j=1}^t \alpha_{t,j}^{\text{LC}} \mathbf{h}_j \quad (32)$$

#### 4.3.3 Global self-attention RNN model

The global self-attention is abstracted from Vaswani et al. [11]'s classic Transformer model. In the additive attention mechanism and Luong's attention mechanisms, the format of 'query' and 'key' varies accordingly, but the third element 'value'  $v$  is hidden and always equal to the output of the RNN model  $\mathbf{h}_j$ . To prevent any misunderstanding, in the previous sections, the calculation of attention output  $\mathbf{z}_t$  directly adopts

the notation  $h_j^{(2)}$  to multiply the attention weights  $\alpha_{t,j}$ . However, in the self-attention mechanism, the element  $v$  has its variable format. Specifically,

$$\mathbf{q}_t = \mathbf{W}_q \mathbf{h}_t^{(2)}, \quad \mathbf{k}_j = \mathbf{W}_k \mathbf{h}_j^{(2)}, \quad \mathbf{v}_j = \mathbf{W}_v \mathbf{h}_j^{(2)} \quad (33)$$

where  $\mathbf{W}_q, \mathbf{W}_k, \mathbf{W}_v \in \mathbb{R}^{d_{RNN} \times d_{RNN}}$  are learnable parameter matrix for the query  $\mathbf{q}_t$ , key  $\mathbf{k}_j$  and  $\mathbf{v}_j$ . And  $h_j^{(2)} \in \mathbb{R}^{d_{RNN}}$  is the output at time  $j$  of the RNN structure. For each time step  $t$  and  $j$ , the attention score  $e_{t,j}$  can be computed through Equation (34).

$$e_{t,j} = \frac{1}{\sqrt{d_{RNN}}} \mathbf{q}_t^\top \mathbf{k}_j \quad (34)$$

It requires a causal mask for preventing future information leak,

$$e_{t,j} = \begin{cases} \frac{1}{\sqrt{d_{RNN}}} \mathbf{q}_t^\top \mathbf{k}_j, & j \leq t \\ -\infty, & j > t \end{cases} \quad (35)$$

Similar to previous attention mechanisms, the attention weights are computed via a softmax function, and the attention output can be computed based on the attention weights.

$$\alpha_{t,j} = \frac{\exp(e_{t,j})}{\sum_{i=1}^t \exp(e_{t,i})} \quad (36)$$

$$\mathbf{z}_t = \sum_{j=1}^t \alpha_{t,j} \mathbf{v}_j \quad (37)$$

#### 4.3.4 Sliding window sparse attention mechanism

Sliding window sparse attention belongs to the self-attention family, and it is first proposed by Beltagy et al. [12]. Like other sparse attention mechanisms, it is developed for capturing the longer-term temporal dependency of the sequential data and lowering the computational cost of global attention mechanisms such as Bahdanau’s attention [30], Luong’s attention [31] and Vaswani’s self-attention [11]. The difference between the sliding window attention and Vaswani’s self-attention is Vaswani’s self-attention calculates the difference between any two time steps, but the sliding window attention of Beltagy et al. [12]’s only calculates the difference between one time step and a range of time steps close to that time step. Figure 4 shows the difference between Vaswani’s self-attention and sliding window sparse attention with causal masks for time series data. The left panel of Figure 4 shows an example of a sliding window sparse attention mechanism when the attention window is equal to 4, and the right panel shows the global self-attention mechanism from Vaswani et al. [11]. The global self-attention calculates the difference between the series at time step  $t$  and all available time steps previous to  $t$ , but the sliding window sparse attention only measures the difference

between the series at time step  $t$  and available time steps previous to  $t$  up to the restrictions of the attention window, which is  $t - 3$  in this example.

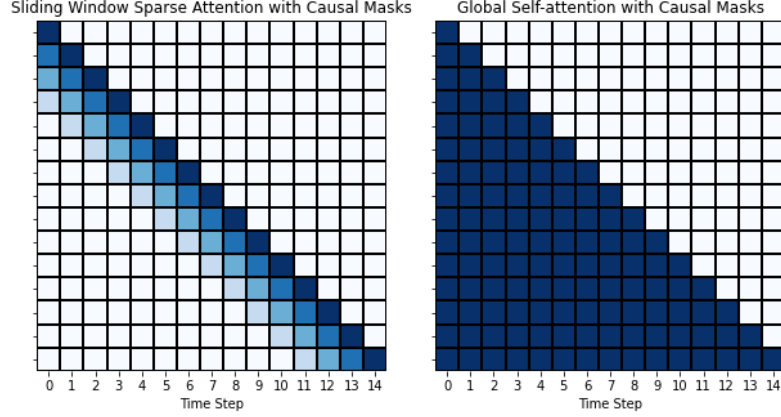


**Fig. 4:** The comparison of sliding window sparse attention and global self attention (with causal masks). This is an example when the attention window is equal to 4. The white grids in both panels represent the time points with causal masks, which means they are not in the calculation of attention weights.

The sliding window sparse attention is developed from the global self-attention, which is shown in Figure 5. Mathematically, to each time step  $t$ , defining the attention window  $\mathcal{S}_t = \{s \mid \max(0, t - w) \leq s \leq t\}$ ,  $s$  is the time step previous to time  $t$ . Thus, the query (q), key (k) and value (v) here of sliding window sparse attention in time step  $t$  and  $s$  are:

$$q_t = W_q h_t, \quad k_s = W_k h_s, \quad v_s = W_v h_s \quad (38)$$

where  $h_t, h_s \in \mathbb{R}^{d_{RNN}}$  are the output from RNN second hidden layer at time  $t$  and  $s$  respectively.  $W_q, W_k, W_v \in \mathbb{R}^{d_{RNN} \times d_{RNN}}$  are the learnable weight matrices of  $q_t, k_s, v_s$ . Therefore, the attention score between time  $t$  and  $s$  can be:

$$\alpha_{t,s} = \frac{\exp(q_t^\top k_s / \sqrt{d_{RNN}})}{\sum_{j \in \mathcal{S}_t} \exp(q_t^\top k_j / \sqrt{d_{RNN}})} \quad (39)$$

Further, the attention output of time  $t$  denoted as  $z_t$  can be:

$$z_t = \sum_{s \in \mathcal{S}_t} \alpha_{t,s} v_s \quad (40)$$

Due to the limited data size of this study, the proposed model only considers the single-head sliding window sparse attention. With the attention window, the computational cost of this attention becomes  $O(T \times \mathcal{S}_t \times d_{RNN})$ .



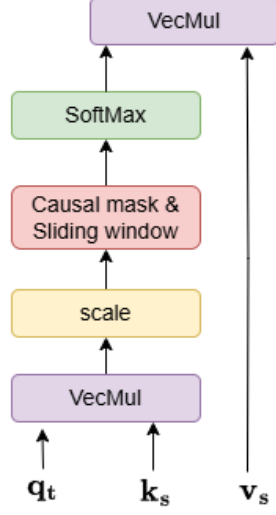


**Fig. 5:** Sliding window sparse attention mechanism workflow diagram.  $q_t, k_s, v_s \in \mathbb{R}^{d_{RNN}}$  are query, key, value at time  $t$  and  $s$  respectively. 'VecMul' is denoted as the vector-wise multiplication.

The main difference between the classic Transformer model [11] and the Longformer model [12] is that the latter employs the assembled attention mechanism which encompasses sparse attention of sliding window attention, dilated sliding window attention (optional) and global attention. For simplifying the model structure for the temporal sparse data, such as the monthly stock pricing data, the proposed model only deploys the sliding window sparse attention layer from the Longformer model and assembles it on an RNN frame for a better capture of the temporal longer-term dependency that exists in the stock pricing data.

To summarize, the calculation of attention output follows the procedure of computing the attention scores, applying the softmax function on attention scores for generating the attention weights and utilizing attention weights multiplies the 'value' for the attention output.

#### 4.4 Linear output of the RNN attention models

Finally, the attention outputs are utilized to compute the estimated label through the linear function. It is shown in Equation (65), where  $\hat{y}_t$  is the linearly estimated label which is the excess return of an individual stock at time  $t$ .

$$\hat{y}_t = \mathbf{W}_{\hat{y}_t} \mathbf{z}_t + b_{\hat{y}_t}, \quad \hat{y}_t \in \mathbb{R} \quad (41)$$

## 4.5 Long short-term memory (LSTM) and Gated recurrent unit (GRU)

The RNN variation models, LSTM and GRU, serve as benchmark models in this study. Due to the gradient explosion and vanishing issues that exist in the naive RNN model, which was suggested by Bengio et al. [37], Hochreiter and Schmidhuber [9] proposes the first LSTM model for capturing a longer dependency of sequential data. They design the input gate, output gate, and cell structure, and embed them in the naive RNN framework to moderate the gradient explosion and vanishing issues. It is improved by Gers et al. [38], who adds a forget gate in the previous LSTM structure. This LSTM is the most commonly applied LSTM in the literature of different domains. Further, people find LSTM is over-parameterized since it has three gates, one cell and one hidden state, albeit it moderates the gradient explosion and vanishing issues to a degree. Thus, Cho et al. [10] proposes the GRU which simplifies the structure of LSTM. GRU only configure two gates: update gate and reset gate, which highly reduces the parameters of a recurrent neural network model. In the early stage, LSTM was developed for speech recognition, sequential labelling, time-series forecasting and handwritten character recognition, while GRU was developed for machine translation originally. However, researchers have proven that GRU performs similarly to LSTM in prediction accuracy from different angles [39–41], especially in the time-series forecasting context. Figure 6 exhibits the entire workflow of the two-layer LSTM adopted in this study from a bird’s-eye view. The first LSTM or GRU layer (‘LSTM/GRU 1’) contains 64 neurons; thus, the dimension of the first layer is 64. And the second LSTM or GRU layer (‘LSTM/GRU 2’) contains 32 neurons, which indicates the dimension of the second LSTM or GRU layer is 32. For time-series forecasting tasks, both LSTM and GRU frame connect a linear layer as the output layer.

Briefly, a two-layer LSTM with distinctive neuron numbers can be mathematically presented as:

$$\mathbf{i}_t^{(1)} = \sigma(W_i^{(1)}\mathbf{x}_t + U_i^{(1)}\mathbf{h}_{t-1}^{(1)} + \mathbf{b}_i^{(1)}) \quad (42)$$

$$\mathbf{f}_t^{(1)} = \sigma(W_f^{(1)}\mathbf{x}_t + U_f^{(1)}\mathbf{h}_{t-1}^{(1)} + \mathbf{b}_f^{(1)}) \quad (43)$$

$$\mathbf{o}_t^{(1)} = \sigma(W_o^{(1)}\mathbf{x}_t + U_o^{(1)}\mathbf{h}_{t-1}^{(1)} + \mathbf{b}_o^{(1)}) \quad (44)$$

$$\tilde{\mathbf{c}}_t^{(1)} = \tanh(W_c^{(1)}\mathbf{x}_t + U_c^{(1)}\mathbf{h}_{t-1}^{(1)} + \mathbf{b}_c^{(1)}) \quad (45)$$

$$\mathbf{c}_t^{(1)} = \mathbf{f}_t^{(1)} \odot \mathbf{c}_{t-1}^{(1)} + \mathbf{i}_t^{(1)} \odot \tilde{\mathbf{c}}_t^{(1)} \quad (46)$$

$$\mathbf{h}_t^{(1)} = \mathbf{o}_t^{(1)} \odot \tanh(\mathbf{c}_t^{(1)}) \quad (47)$$

Where  $\mathbf{i}_t^{(1)}$ ,  $\mathbf{f}_t^{(1)}$  and  $\mathbf{o}_t^{(1)}$  are input gate, forget gate and output gate of the first layer, respectively.  $\tilde{\mathbf{c}}_t^{(1)}$  and  $\mathbf{c}_t^{(1)}$  are candidate cell state and cell state respectively.  $\sigma(\cdot)$  is the activation function, sigmoid in this case, and  $\tanh(\cdot)$  is the hyperbolic tangent function; it serves as the activation function as well.  $W_i^{(1)}$ ,  $W_f^{(1)}$ ,  $W_o^{(1)}$ ,  $W_c^{(1)} \in \mathbb{R}^{d_1 \times d_{in}}$  and  $U_i^{(1)}$ ,  $U_f^{(1)}$ ,  $U_o^{(1)}$ ,  $U_c^{(1)} \in \mathbb{R}^{d_1 \times d_1}$  are learnable parameter matrices for each gate

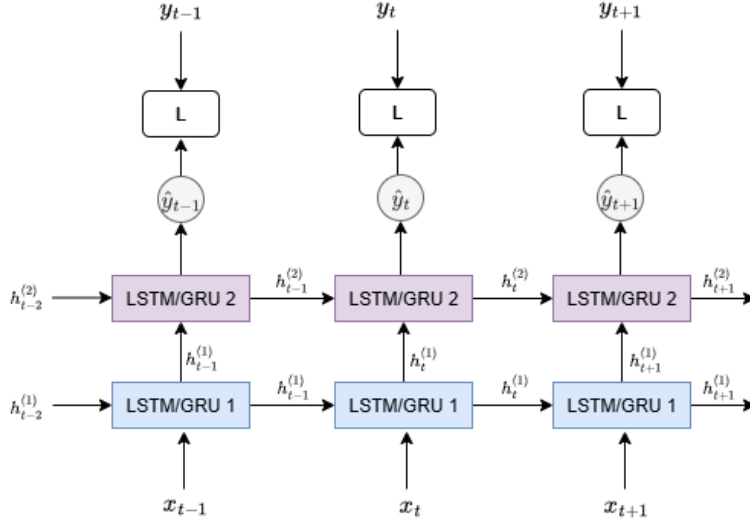


**Fig. 6:** Entire workflow chart for two-layer LSTM and GRU model.  $x$  is the abstracted factors from the MLP pretraining process, while  $h$  is the output from the LSTM or GRU layer.  $\hat{y}$  is the estimated output from the linear layer, and  $L$  means the loss function.  $y$  is the actual value of the label, the stock excess returns in this case.

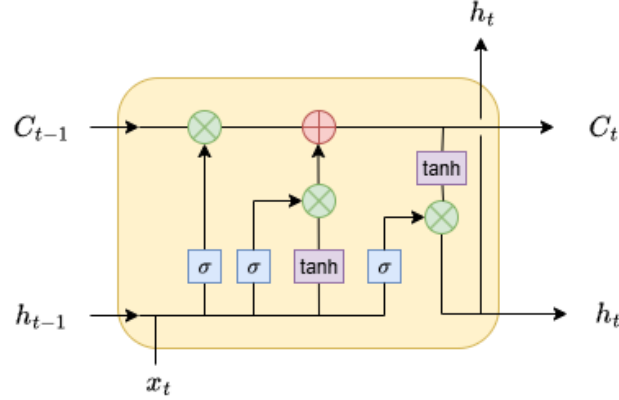


**Fig. 7:** The mechanism inside a LSTM layer. Where  $C$  and  $h$  are the cell state and the hidden state, respectively, and  $x$  is the abstracted factors from the pretraining process.  $\sigma$  indicates the activation function of sigmoid, while  $\tanh$  is the hyperbolic tangent function. The red dot and green dots depict the addition operation and multiplication, respectively.

and cell, where  $d_1$  is dimension of first layer (equal to neuron number) and  $d_{in}$  indicates the dimension of the input.  $\mathbf{b}_i^{(1)}, \mathbf{b}_f^{(1)}, \mathbf{b}_o^{(1)}, \mathbf{b}_c^{(1)} \in \mathbb{R}^{d_1}$  are the biases for each gate and cell. The second layer of LSTM has a similar structure to the first layer. For the input gate, forget gate, output gate and candidate cell, the original input  $\mathbf{x}_t$  is substituted by the first layer output  $\mathbf{h}_t^{(1)}$ . And the  $\odot$  is the sign of the Hadamard product. Figure 7 shows the mechanism inside a LSTM layer.

Equation (48) to Equation (53) show the mechanism of the LSTM second layer. The gates and cells computation relies on the output of the first layer and the previous output of the second layer. The  $\mathbf{h}_t^{(2)}$  is the final hidden state that will be passed to the linear output layer for deriving the estimated label  $\hat{\mathbf{y}}_t$ , the estimated stock excess return at time  $t$  in this case, which is presented in Equation (62).

$$\mathbf{i}_t^{(2)} = \sigma(W_i^{(2)}\mathbf{h}_t^{(1)} + U_i^{(2)}\mathbf{h}_{t-1}^{(2)} + \mathbf{b}_i^{(2)}) \quad (48)$$

$$\mathbf{f}_t^{(2)} = \sigma(W_f^{(2)}\mathbf{h}_t^{(1)} + U_f^{(2)}\mathbf{h}_{t-1}^{(2)} + \mathbf{b}_f^{(2)}) \quad (49)$$

$$\mathbf{o}_t^{(2)} = \sigma(W_o^{(2)}\mathbf{h}_t^{(1)} + U_o^{(2)}\mathbf{h}_{t-1}^{(2)} + \mathbf{b}_o^{(2)}) \quad (50)$$

$$\tilde{\mathbf{c}}_t^{(2)} = \tanh(W_c^{(2)}\mathbf{h}_t^{(1)} + U_c^{(2)}\mathbf{h}_{t-1}^{(2)} + \mathbf{b}_c^{(2)}) \quad (51)$$

$$\mathbf{c}_t^{(2)} = \mathbf{f}_t^{(2)} \odot \mathbf{c}_{t-1}^{(2)} + \mathbf{i}_t^{(2)} \odot \tilde{\mathbf{c}}_t^{(2)} \quad (52)$$

$$\mathbf{h}_t^{(2)} = \mathbf{o}_t^{(2)} \odot \tanh(\mathbf{c}_t^{(2)}) \quad (53)$$

where  $W_i^{(2)}, W_f^{(2)}, W_o^{(2)}, W_c^{(2)} \in \mathbb{R}^{d_2 \times d_1}$  and  $U_i^{(2)}, U_f^{(2)}, U_o^{(2)}, U_c^{(2)} \in \mathbb{R}^{d_2 \times d_2}$  are the learnable parameter matrices of each gate and cell, where  $d_2$  is the dimension of the second layer (equal to neuron number of the second layer).  $\mathbf{b}_i^{(2)}, \mathbf{b}_f^{(2)}, \mathbf{b}_o^{(2)}, \mathbf{b}_c^{(2)} \in \mathbb{R}^{d_2}$  are the bias vectors for each gate and cell.

GRU simplifies the LSTM by substituting the input gate, forget gate, output gate and cell states system with the update gate and reset gate system. Equation (54) to Equation (61) shows the mathematical presentation of the two-layer GRU. Similar to LSTM, GRU employs a gated system to control the memory length. It removes the cell states of LSTM but embeds the candidate hidden state for a substitution of candidate cell state of LSTM which highly reduces the parameter numbers. In the first GRU layer, the updated gate and reset gate are computed according to the inputs and previous hidden states with the sigmoid activation function. The candidate hidden state is computed through the input and reset gated previous hidden state with the hyperbolic tangent activation function. The output hidden state is computed via update gated hidden state and candidate hidden state. Subsequently, the hidden state computed from the first layer is passed to the second layer for the process to compute the final hidden state which is for derivation of estimated label  $\hat{\mathbf{y}}_t$  through a linear function shows in Equation (62). Figure 8 illustrates the mechanism of a GRU layer.

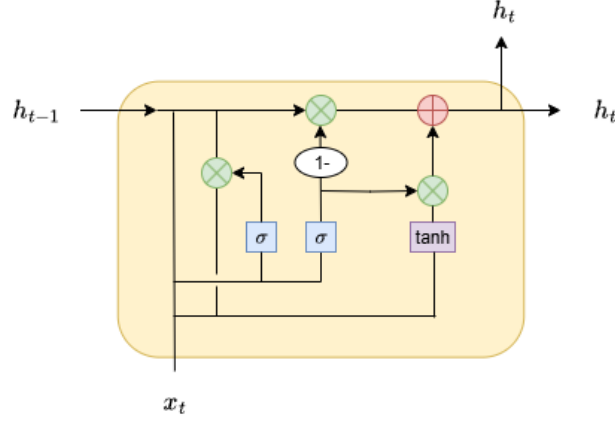


**Fig. 8:** The mechanism inside a GRU layer. Where  $h$  is the hidden state, and  $x$  is the abstracted factors from the pretraining process.  $\sigma$  indicates the activation function of sigmoid, while  $\tanh$  is the hyperbolic tangent function. The red dot and green dots depict the addition operation and multiplication, respectively.

$$\mathbf{up}_t^{(1)} = \sigma(W_{up}^{(1)} \mathbf{x}_t + U_{up}^{(1)} \mathbf{h}_{t-1}^{(1)} + \mathbf{b}_{up}^{(1)}) \quad (54)$$

$$\mathbf{re}_t^{(1)} = \sigma(W_{re}^{(1)} \mathbf{x}_t + U_{re}^{(1)} \mathbf{h}_{t-1}^{(1)} + \mathbf{b}_{re}^{(1)}) \quad (55)$$

$$\tilde{\mathbf{h}}_t^{(1)} = \tanh(W_h^{(1)} \mathbf{x}_t + U_h^{(1)} (\mathbf{re}_t^{(1)} \odot \mathbf{h}_{t-1}^{(1)}) + \mathbf{b}_h^{(1)}) \quad (56)$$

$$\mathbf{h}_t^{(1)} = (1 - \mathbf{up}_t^{(1)}) \odot \mathbf{h}_{t-1}^{(1)} + \mathbf{up}_t^{(1)} \odot \tilde{\mathbf{h}}_t^{(1)} \quad (57)$$

Equation (54) to Equation (57) shows the mechanism of the first GRU layer, where  $\mathbf{up}_t^{(1)}$  and  $\mathbf{re}_t^{(1)}$  represent the update gate and reset gate respectively.  $\tilde{\mathbf{h}}_t^{(1)}$  is denoted as the candidate hidden state and  $\mathbf{h}_t^{(1)}$  is the notation of hidden state output.  $W_{up}^{(1)}, W_{re}^{(1)}, W_h^{(1)} \in \mathbb{R}^{d_1 \times d_{in}}$  and  $U_{up}^{(1)}, U_{re}^{(1)}, U_h^{(1)} \in \mathbb{R}^{d_1 \times d_1}$  are the learnable parameter matrices of gates and hidden states, while  $\mathbf{b}_{up}^{(1)}, \mathbf{b}_{re}^{(1)}, \mathbf{b}_h^{(1)} \in \mathbb{R}^{d_1}$  are the biases.  $d_1$  and  $d_{in}$  are the dimension of the first GRU layer and input respectively. Analogous to the first GRU layer, the second GRU layer has an identical configuration apart from changing the input  $\mathbf{x}_t$  to the hidden state of the first GRU layer output  $\mathbf{h}_t^{(1)}$ , which shows in Equation (58) to Equation (61).

$$\mathbf{up}_t^{(2)} = \sigma(W_{up}^{(2)} \mathbf{h}_t^{(1)} + U_{up}^{(2)} \mathbf{h}_{t-1}^{(2)} + \mathbf{b}_{up}^{(2)}) \quad (58)$$

$$\mathbf{re}_t^{(2)} = \sigma(W_{re}^{(2)} \mathbf{h}_t^{(1)} + U_{re}^{(2)} \mathbf{h}_{t-1}^{(2)} + \mathbf{b}_{re}^{(2)}) \quad (59)$$

$$\tilde{\mathbf{h}}_t^{(2)} = \tanh(W_h^{(2)} \mathbf{h}_t^{(1)} + U_h^{(2)} (\mathbf{re}_t^{(2)} \odot \mathbf{h}_{t-1}^{(2)}) + \mathbf{b}_h^{(2)}) \quad (60)$$

$$\mathbf{h}_t^{(2)} = (1 - \mathbf{up}_t^{(2)}) \odot \mathbf{h}_{t-1}^{(2)} + \mathbf{up}_t^{(2)} \odot \tilde{\mathbf{h}}_t^{(2)} \quad (61)$$

Where  $\mathbf{up}_t^{(2)}$  and  $\mathbf{re}_t^{(2)}$  represent the update gate and reset gate in the second GRU layer, while  $\tilde{\mathbf{h}}_t^{(2)}$  and  $\mathbf{h}_t^{(2)}$  are the candidate hidden state and hidden state of the second layer.  $\mathbf{W}_{up}^{(2)}, \mathbf{W}_{re}^{(2)}, \mathbf{W}_h^{(2)} \in \mathbb{R}^{d_2 \times d_1}$  and  $\mathbf{U}_{up}^{(2)}, \mathbf{U}_{re}^{(2)}, \mathbf{U}_h^{(2)} \in \mathbb{R}^{d_2 \times d_2}$  are the learnable parameter matrices of gates and hidden states of the second layer, and  $\mathbf{b}_{up}^{(2)}, \mathbf{b}_{re}^{(2)}, \mathbf{b}_h^{(2)} \in \mathbb{R}^{d_2}$  are the biases of second layer.  $d_2$  is denoted as the dimension of the second layer. Since the LSTM and GRU in this study are in the time-series forecasting context, the linear output layer is assembled for such tasks. Thus, the linear output for RNN and its variation models, the LSTM model and the GRU model, can be presented as:

$$\hat{\mathbf{y}}_t = \mathbf{W}_{\hat{\mathbf{y}}_t} \mathbf{h}_t^{(2)} + \mathbf{b}_{\hat{\mathbf{y}}_t} \quad (62)$$

where  $\mathbf{h}_t^{(2)} \in \mathbb{R}^{d_2}$  is the output hidden state of second LSTM or GRU layer, while  $\mathbf{W}_y \in \mathbb{R}^{d_{out} \times d_2}$  and  $\mathbf{b}_y \in \mathbb{R}^{d_{out}}$  are the parameter matrix and bias of linear layer, where  $d_{out}$  is the output dimension.  $\hat{\mathbf{y}}_t \in \mathbb{R}^{d_{out}}$  is the estimated label  $\hat{\mathbf{y}}_t$  at time  $t$ .

#### 4.6 Estimation

For estimating the main module, RNN with an attention layer, of the proposed model, the MSE function is selected as the loss function, and the L1 norm is added to the loss function as a regularization penalty. Concretely, it can be presented as:

$$\mathcal{L} = \frac{1}{T} \sum_{t=1}^T (y_t - \hat{y}_t)^2 + \lambda \|\mathbf{W}\|_1 \quad (63)$$

where  $\mathcal{L}$  is denoted as loss function,  $T$  is the length of the entire time window and  $y_t$  is the actual value of the label at time  $t$ .  $\mathbf{W}$  represents all parameters in the model, and  $\lambda$  is the regularization coefficient which requires pre-setting. The best parameters for prediction can be derived from minimizing the loss function via the stochastic gradient descent (SGD) method or the adaptive moment estimation (Adam) optimizer for improving the model training efficiency and mitigating gradient explosion and vanishing problems. The SGD and Adam optimizer are recruited for the estimation task, which is shown in the **Appendix**.

$$\mathbf{W}^* = \arg \min_{\mathbf{W}} \left\{ \frac{1}{T} \sum_{t=1}^T (y_t - \hat{y}_t)^2 + \lambda \|\mathbf{W}\|_1 \right\} \quad (64)$$

Equation (64) depicts how to derive the best parameters from minimizing the MSE loss function, where  $\mathbf{W}^*$  is denoted as the best parameters selected for forecasting.

#### 4.7 Forecasting

One-step ahead forecasting for the RNN attention models can be derived from Equation (65)

$$\hat{\mathbf{y}}_{t+1} = \mathbf{W}_{\hat{\mathbf{y}}_t} \mathbf{z}_{t+1} + \mathbf{b}_{\hat{\mathbf{y}}_t} \quad (65)$$

And the one-step ahead forecasting for the RNN, LSTM and GRU models is

$$\hat{y}_{t+1} = \mathbf{W}_{\hat{y}_t} \mathbf{h}_{t+1}^{(2)} + b_{\hat{y}_t} \quad (66)$$

It applies the best weights and biases to the outputs from the main models to derive the estimated stock excess return at time  $t + 1$ .

## 5 Empirical results

In this section, the proposed models and benchmark models are compared from two angles: model-wise and trading strategy-wise. Model-wise performance is measured by the mean of 420 stocks' the out-of-sample (OOS) coefficient of determination ( $R_{OOS}^2$ ), mean square error (MSE), alpha and its statistics, which are shown in Table 2. The algorithms of these indicators are presented in Equation (67) to Equation (69).

$$R_{\text{oos}}^2 = 1 - \frac{\sum (r_{i,t+1} - \hat{r}_{i,t+1})^2}{\sum (r_{i,t+1} - \bar{r}_{\text{train}})^2} \quad (67)$$

$$MSE = \frac{1}{TN} \sum_{t=1}^T (r_{i,t} - \hat{r}_{i,t})^2 \quad (68)$$

$$\alpha_{\text{avg}} := \frac{1}{N} [E(r_{i,t}) - E(\hat{r}_{i,t})] \quad (69)$$

Where  $r_{i,t+1}$  are the real out-of-sample excess returns,  $\hat{r}_{i,t+1}$  is the predicted excess returns, which is equal to  $\hat{y}_{t+1}$  in Section 4 and  $\bar{r}_{\text{train}}$  is the mean of the excess returns in the training period.  $i$  indicates the stock  $i$ , and  $TN$  is the time length observation number multiplied by the number of stocks. Here, alpha is the OOS average estimation error in model evaluation, but it has the specific meaning in the asset pricing context.

In the traditional asset pricing concept,  $\alpha$  is the intercept of a linear factor model. It means the risk-adjusted return of a stock. If the  $\alpha = 0$ , the stock excess return is perfectly explained by the selected or constructed factors; if  $\alpha > 0$ , it indicates the extra capital gain exists after controlling the risks brought by factors, which is also known as the 'arbitrage opportunities'; if  $\alpha < 0$ , it implies the stock underperform the model's prediction. The latter two circumstances indicate the existence of pricing errors, but practitioners chase the positive  $\alpha$  as the abnormal returns beyond the factors. In traditional asset pricing literature, those with a linear model frame, factor exploration research pursues  $\alpha$  approaching zero to verify that their factors can perfectly explain the asset returns, which satisfies the non-arbitrage hypothesis. That is slightly different in ML-based asset pricing literature, especially in this case. The linear output layer, which is shown in Equation (65) and Equation (62), still makes the asset pricing model explainable, but forces the restriction of the non-arbitrage condition by removing the intercept term of  $\alpha$ . The computation of  $\alpha$  for the ML-based asset pricing is also known as residual  $\alpha$ , which is employed by Gu et al. [3], Ma et al. [26] and is shown in Equation (69). That means if the assumption stands for

the linear output layer form, the mean of both pricing error  $\alpha$  and model bias  $\mathbf{b}$  should be equal to zero; otherwise, it implies that the  $\alpha$ , the abnormal return or the arbitrage opportunity exists, or there are unexplored factors. Exploring the structure of  $\alpha$ , how to minimise  $\alpha$ , and the relation to the bias of the ML frame are interesting directions for future research.

The Diebold-Mariano (DM) [42] test is adopted for evaluating the difference between models in this study. Equation (70) to Equation (72) presents the mechanism of the DM test. DM test here using the Mean Absolute Error (MAE) as the foundation for its robustness compared with the MSE option. MAE is less sensitive to outliers than MSE, which is particularly suitable for financial time series in AI models that contain more complicated and variable structure in their prediction errors (e.g. non-Gaussian, heavy-tailed, etc.). Therefore, MAE-DM here reflects typical difference forecasting performance and avoids being affected by a few large deviations causes false detection of the difference between models. Hence, MAE-DM statistics provide a more realistic and reliable assessment of model superiority in this study.

$$d_{t+1} = \frac{1}{h} \sum_{i=1}^h \left( |e_{i,t+1}^{(m)}| - |e_{i,t+1}^{(n)}| \right) \quad (70)$$

$$\bar{d} = \frac{1}{T} \sum_{t=1}^T d_{t+1} \quad (71)$$

$$DM_{\text{statistics}} = \frac{\bar{d}}{d_{\text{standard error}}} \quad (72)$$

where  $|e_{i,t+1}^{(m)}|$ ,  $|e_{i,t+1}^{(n)}|$  are the absolute value of forecasting errors derived from  $(r_{i,t+1} - \hat{r}_{i,t+1})$  of model  $m$ ,  $n$  respectively.  $i$  indicates the stock  $i$ .  $h$  is the stock number which is 420 in our case.  $d_{t+1}$  is the cross-sectional average difference between model  $m$  and model  $n$  absolute forecasting errors,  $\bar{d}$  is the mean of  $d_{t+1}$ ,  $d_{\text{standard error}}$  is the standard error of  $d_t$ .

For a greater interpretation of the model, this study also calculates the factor importance for the MLP autoencoder abstracted factors and the correlation between the abstracted factors and the original factors. Due to space limitations, the factor correlation heatmaps of the proposed models and the variable importance of the models are presented in the appendix. Mathematically, the permutation variable importance (VI) can be exhibit as:

$$L_{\text{baseline}} = \mathcal{L}(r_{i,t}, f(X)) \quad (73)$$

$$L_{\text{perm}}(X_i) = \mathcal{L}(r_{i,t}, f(X_{\text{perm}})) \quad (74)$$

$$\text{Importance}(X_i) = L_{\text{perm}}(X_i) - L_{\text{baseline}} \quad (75)$$



where  $L_{baseline}$  is baseline loss or original out-of-sample loss,  $X$  is the original feature matrix, and  $f(\cdot)$  is the model forms.  $L_{perm(X_i)}$  is the loss that an individual feature  $X_i$  is permuted. Then, the importance of  $X_i$  is equal to the difference between the permuted loss and the baseline loss.

This study uses the trend-following sign signal trading strategy as the market timing approach, and the transaction cost is configured as 50 base points by referring literature [26]. For measuring the trading strategy-wise performance, it follows the traditional asset pricing indicators, which are annualized returns, Sharpe ratio, Sortino ratio and maximum drawdown (MDD). Equation (76) to Equation (79) presents the calculation of these indicators.

$$Annualized\ Return = \left\{ 1 + \left[ \prod_{i=1}^n (1 + r_{i,t}) - 1 \right]^{\frac{12}{n}} \right\} - 1 \quad (76)$$

$$Sharpe\ Ratio = \frac{E(r_p) - r_f}{\sigma_p} \quad (77)$$

$$Sortino\ Ratio = \frac{E(r_p) - r_f}{\sigma_d} \quad (78)$$

$$Maximum\ Drawdown = \max_{t \in [0, T]} \left( \frac{c_{\max}(t) - c(t)}{c_{\max}(t)} \right) \quad (79)$$

where  $n$  is the number of the observations,  $E(r_p)$  is the expected portfolio return and  $r_f$  represents the risk-free rate.  $\sigma_p$  and  $\sigma_d$  are the portfolio and portfolio downside standard deviation, respectively.  $C_{\max}(t)$  is the highest value during time  $t$ , and  $C(t)$  is the value at time  $t$ . For a better comparison of models that perform under the extreme market fluctuation caused by the COVID-19 pandemic, all results are displayed in three periods: period without pandemic ('1911'), period containing pandemic ('2112') and period containing pandemic and one-year pandemic recovery period ('2212'). Figure E5 is the price index of the three periods, which depicts the market fluctuations during the three periods. Concretely, Period '1911' includes a mild uptrend, Period '2112' encompasses Period '1911' plus a volatile but sharp uptrend, and Period '2212' covers Period '2112' plus a phase with no significant trend but extreme volatile sideways movement.

## 5.1 Model performance

Table 2 displays the model performance indicators for all periods. It includes the average OOS  $R^2$ ,  $MSE$ ,  $\alpha$  and its t-statistics to show whether it is significantly different from zero. From the average OOS  $R^2$  of Period '1911', which indicates the out-of-sample fitness of the models, we can see that only RNN Luong's dot product attention (LD), vanilla RNN, RNN global self-attention (self) and RNN sliding window sparse attention model have positive OOS  $R^2$  values. The alternatives have negative values, which implies these models contain overfitting issues. Surprisingly, the vanilla RNN model obtains the highest OOS  $R^2$ , which is 10.28% in Period '1911', followed by



**Fig. 9:** Market-cap-weighted (MC) Price Index.

the RNN global self-attention model (1.63%) and the RNN sliding window attention model (1.28%). In Period '2112', all models' fitness is improved slightly, apart from the proposed RNN attention models. The RNN self-attention model, its OOS  $R^2$  drops noticeably to 1.2%, which is worse than the RNN sliding window sparse attention (1.12%). Model GRU's  $R^2$  increases considerably from -0.29% to 0.89%, which follows the best-performed models: vanilla RNN model, RNN global self-attention model and RNN sliding window sparse attention model. For Period '2212', the vanilla RNN model remains the model with the highest OOS  $R^2$  value, which is 13.77% followed by the RNN global attention model (1.28%). However, GRU's  $R^2$  continuously increases, and it becomes slightly higher than the RNN sliding window attention model (1.02%). By comparing across the three periods, the negative  $R^2$  values of Model RNN additive attention ('Batt'), RNN Luong's concatenate (LC) attention and LSTM demonstrate model overfitting to some extent. Apart from vanilla RNN model, the rest of the models show relatively stable fitness during the large market fluctuation. The vanilla RNN exhibits great fitness during the extreme market conditions, even better than the fitness in the pre-pandemic period which contains a mild uptrend. Average OOS MSE agrees with the findings from the average OOS  $R^2$ .

Figure 10 and Figure 11 are the OOS  $R^2$  and MSE distribution plots of models with the best OOS fitness. The OOS  $R^2$  distribution plots show that the vanilla RNN model has the majority of stocks with the positive OOS  $R^2$  during all periods, where they are distributed between 0 to 0.45. There are some similarities between the distribution of the RNN global self-attention and the RNN sliding window attention model: more than 60% of the stocks have the positive OOS  $R^2$  values, and both of them are right-skewed in all periods. However, the RNN sliding window attention model has longer right tails than the RNN global attention model, which indicates

Model	avg_ $R^2$	avg_MSE	avg_ $\alpha$	Ann_avg_ $\alpha$	t_statistic
<b>1911</b>					
Batt	-0.0056	0.0060	0.0035	0.0417	9.4624***
GRU	-0.0029	0.0060	0.0036	0.0429	9.5687***
LC	-0.0105	0.0061	0.0035	0.0423	9.5809***
LD	0.0009	0.0060	0.0035	0.0426	9.4785***
LG	-0.0053	0.0060	0.0037	0.0450	10.2364***
LSTM	-0.0075	0.0060	0.0038	0.0455	10.2192***
RNN	0.1028	0.0053	0.0040	0.0478	10.5572***
self_att	0.0163	0.0059	0.0028	0.0340	7.9699***
sparse_att	0.0128	0.0059	0.0030	0.0363	8.5817***
<b>2112</b>					
Batt	-0.0041	0.0080	0.0053	0.0632	16.5328***
GRU	0.0089	0.0079	0.0049	0.0586	14.3459***
LC	-0.0073	0.0080	0.0053	0.0632	15.8036***
LD	0.0019	0.0079	0.0053	0.0641	16.5363***
LG	-0.0027	0.0080	0.0054	0.0645	17.0102***
LSTM	-0.0060	0.0080	0.0055	0.0660	17.2300***
RNN	0.1327	0.0068	0.0039	0.0467	11.7454***
self_att	0.0120	0.0078	0.0045	0.0540	14.2660***
sparse_att	0.0112	0.0079	0.0048	0.0581	15.3381***
<b>2212</b>					
Batt	-0.0004	0.0084	0.0038	0.0453	13.0552***
GRU	0.0115	0.0083	0.0036	0.0429	11.7015***
LC	-0.0034	0.0084	0.0038	0.0456	13.1388***
LD	0.0037	0.0083	0.0039	0.0473	13.4858***
LG	0.0007	0.0084	0.0039	0.0469	13.8141***
LSTM	-0.0018	0.0084	0.0040	0.0480	14.3907***
RNN	0.1377	0.0071	0.0025	0.0303	8.5837***
self_att	0.0128	0.0083	0.0038	0.0461	13.7656***
sparse_att	0.0102	0.0083	0.0035	0.0416	11.8082***

**Table 2:** Out-of-sample Predictive indicators and  $\alpha$ . 'Ann' is the notation of annualization, and 'avg' is short for 'average'. \*, \*\* and \*\*\* depict the statistical significance level of 90%, 95% and 99% respectively.

that these anomalies may lift the average OOS  $R^2$  value in Table 2. That implies that the RNN global self-attention model performs more stably on individual stocks than the RNN sliding window attention model during all periods. The MSE distribution plots agree with the findings from the OOS  $R^2$  distribution plots.

All models have significant positive average  $\alpha$ s during all periods. This demonstrates the persistence of the extra capital gain beyond the factors. Economically, this indicates that there are excess returns that cannot be fully explained by the factors, which

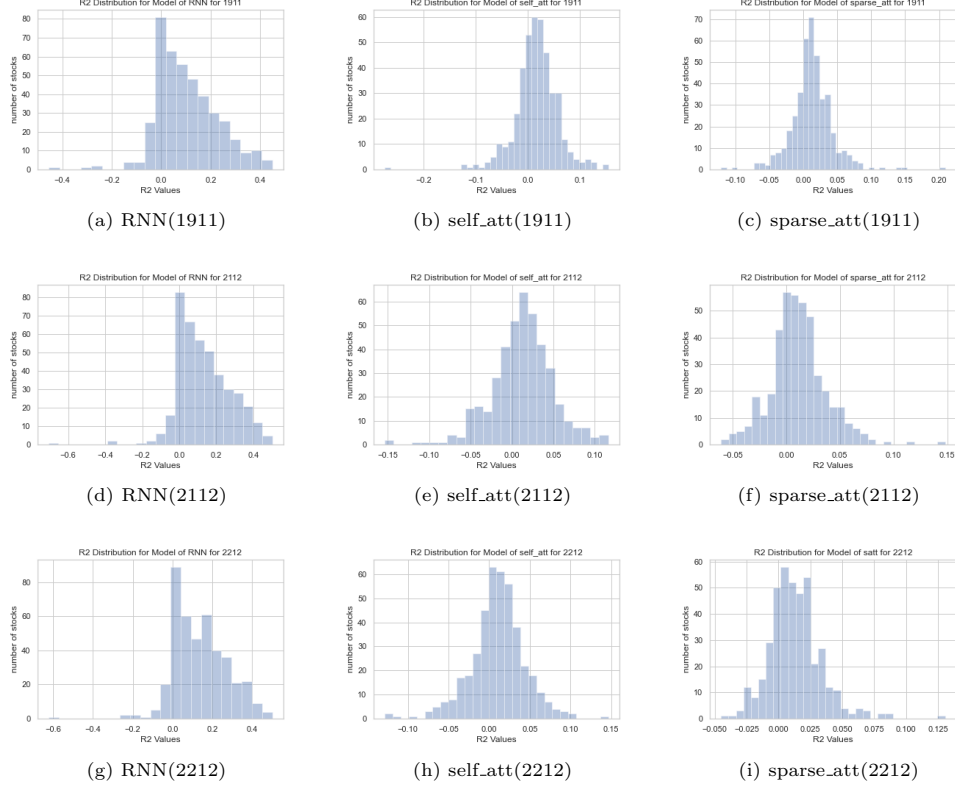


**Fig. 10:** Out-of-sample  $R^2$  distribution of the best fitted models

implies the unexplored or omitted factors or the existence of persistent arbitrage opportunities in the market, but it is unlikely to be caused by model misspecification. Three reasons stand for this interpretation. Firstly, the notably high  $\alpha$  values observed during the '2112' period were characterized by a sharp market uptrend, which likely contributed to the model's tendency to underpredict returns systematically. In contrast, the relatively moderate  $\alpha$  values in '1911' and '2212'—which correspond to a mild uptrend and a sideways market, respectively—suggest that excess return potential tends to concentrate in more strongly trending environments. Secondly, apart from the vanilla RNN model, there is no incredible difference between the average OOS  $\alpha$  of models in a single period. Thirdly, at least 60% of stocks have positive alpha individually in different models with distinctive periods. An example  $\alpha$  distribution plot is shown in Figure 12. Periodically, the vanilla RNN model has the highest annualized OOS residual  $\alpha$  (4.78%) in Period '1911', while LSTM model has the highest values in Period '2112' (6.6%) and Period '2212' (4.8%). Nevertheless, in each period, the difference between models is modest.

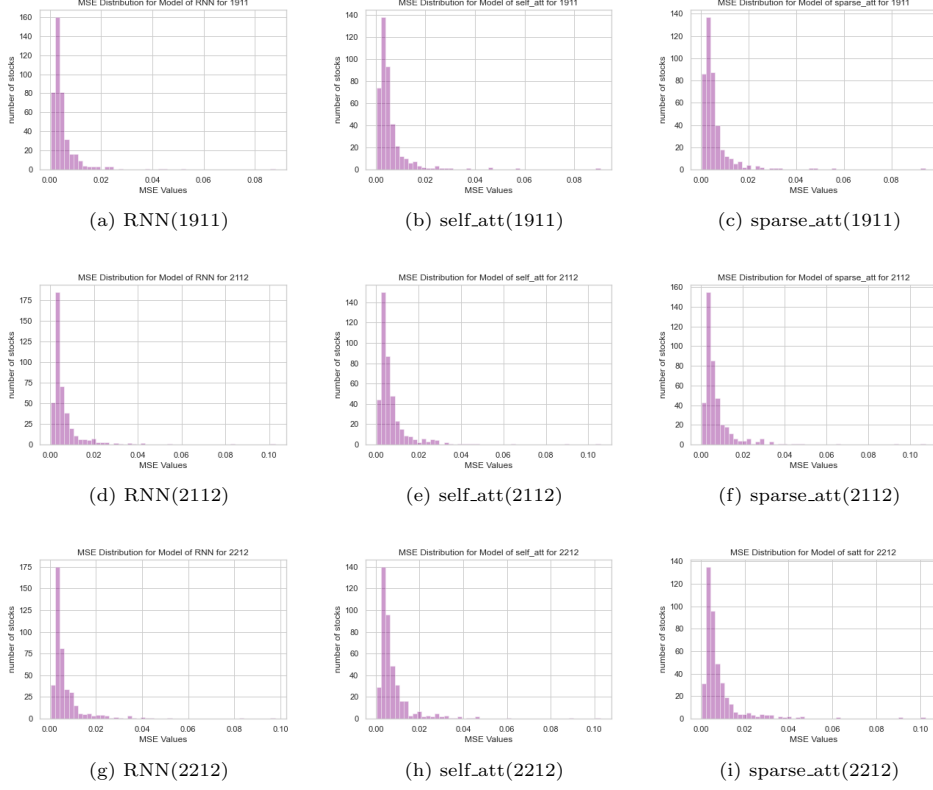


**Fig. 11:** Out-of-sample MSE distribution of the best fitted models

The DM test evaluates the null hypothesis that two competing forecasts have equal predictive accuracy. Table 3 shows the results of the DM test. Numbers in parentheses illustrate negative values. A negative value between two models means the model that shows as the row label outperforms the model that shows as the column label. The DM test results agree with the OOS  $R^2$  results from Table 2. The proposed attention models significantly outperform alternative models in Period 1911, except for the vanilla RNN model. However, the advantage of the proposed models against the GRU and RNN Luong dot product attention model (LD) becomes less pronounced in Period 2112, when the market surged sharply. In Period 2212, when the market experienced a sharp decline followed by a period of sideways movement, the advantage of the proposed RNN global self-attention model (self\_att) nearly vanished, but the advantage of the proposed RNN sliding window attention model (sparse\_att) remains strong. On the other hand, the difference between the proposed models is insignificant. Among the benchmark models, RNN Luong’s concatenate attention model (LC) achieves the worst-performing model during all periods, followed by RNN additive attention model (Batt). RNN LD model, as the foundation of the proposed model, performs significantly better than RNN Luong’s attention model (LG), but shows less advantage in

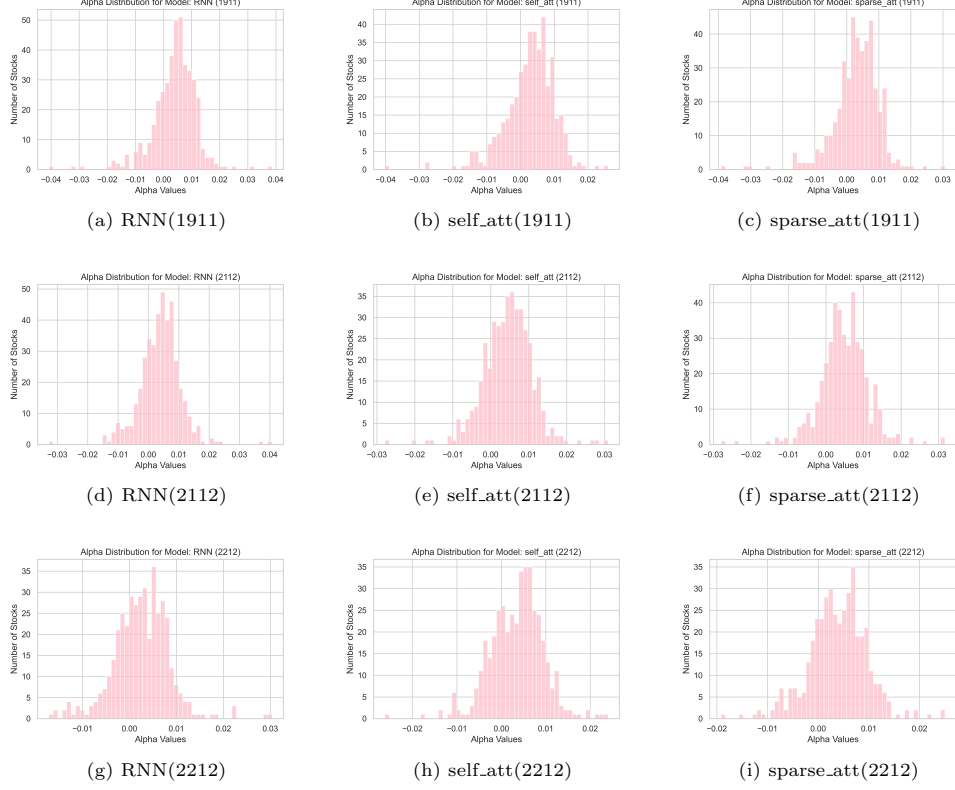


**Fig. 12:** Out-of-sample  $\alpha$  distribution of the best fitted models

the market turbulence period. GRU insignificantly underperforms the RNN LD model in Period 1911, but apart from this, it outperforms all RNN attention models, excluding the proposed models, in all periods. Whereas the LSTM model shows inconsistent performance across time. The overall performance of GRU is better and stable than LSTM.

## 5.2 Back-testing performance

Back-testing refers to the process of evaluating a trading strategy or predictive model by applying it to OOS returns to assess its performance. The predictive models provide the predictive returns; henceforth, a market timing strategy or trading signal generating system would be deployed to the real returns and predictive returns to generate trading signals for guiding trading behaviours (open or close positions). In this study, the sign signal generation method from the typical trend-following trading strategy is adopted for the market timing assignment. Concretely, if the predictive return at a time point is positive, which matches the real return in that time point, the circumstance is considered a buy-side (long) signal. The simulated buy transaction takes place, and the real returns from the next time point would be counted as

<b>1911</b>	Batt	GRU	LC	LD	LG	LSTM	RNN	self_att
GRU	(0.6982)							
LC	2.1446**	2.2629**						
LD	(2.2833)**	(1.1017)	(3.9646)***					
LG	0.6385	1.2206	(1.6562)*	2.7083***				
LSTM	0.6732	1.1140	(2.1312)**	3.0670***	(0.0911)			
RNN	(4.9172)***	(5.1346)***	(5.0906)***	(4.7060)***	(5.0103)***	(4.8731)***		
self_att	(3.0028)***	(2.5439)**	(3.2363)***	(1.9552)*	(3.0329)***	(2.8163)***	4.5544***	
sparse_att	(3.7577)***	(2.7218)***	(3.7399)***	(1.9554)*	(3.3780)***	(3.1863)***	4.3911***	0.4900
<b>2112</b>	Batt	GRU	LC	LD	LG	LSTM	RNN	self_att
GRU	(1.9614)**							
LC	1.5414	2.3673**						
LD	(1.9949)**	0.9794	(2.5013)**					
LG	(1.0047)	1.5095	(2.2068)**	1.1826				
LSTM	(0.0830)	1.7322*	(1.8323)*	1.4175	0.7910			
RNN	(4.4561)***	(4.6877)***	(4.4784)***	(4.4261)***	(4.3622)***	(4.3264)***		
self_att	(2.1551)**	(0.1699)	(2.3836)**	(1.3051)	(1.7610)*	(1.7311)*	4.3884***	
sparse_att	(4.0388)***	(0.3798)	(4.1648)***	(2.2091)**	(3.5716)***	(3.0488)***	4.1145***	(0.3165)
<b>2212</b>	Batt	GRU	LC	LD	LG	LSTM	RNN	self_att
GRU	(1.9705)**							
LC	1.3191	2.3313**						
LD	(2.0331)**	0.9554	(2.4469)**					
LG	(1.2306)	1.4038	(2.3887)**	0.8803				
LSTM	(0.2899)	1.6959*	(1.9967)**	1.2578	0.8789			
RNN	(4.9013)***	(5.1707)***	(4.9105)***	(4.8009)***	(4.7736)***	(4.7618)***		
self_att	(1.4775)	0.6028	(1.7479)*	(0.4179)	(0.8791)	(1.0905)	4.9687***	
sparse_att	(3.6419)***	(0.1641)	(3.6472)***	(1.8012)*	(2.8850)***	(2.6393)***	4.6210***	1.2427

**Table 3:** DM test statistics. Values in parentheses indicate the negative values. A negative value means the model named with the row label outperforms the model with the column label. For example, the first value in the first column of the '1911' panel, which is (0.6982), indicates that Model GRU outperforms Model Batt. \*, \*\* and \*\*\* depict the statistical significance level of 90%, 95% and 99%, respectively.

a gain or loss until the sell-side signal (negative predictive return matches negative real return) shows up as the indicator of closing position. This is also known as the long-only strategy. The short-only strategy is in contrast to the long-only strategy, which opens a short position when both real return and predictive return have negative values at one time point, while closing this position when they both have positive value. The back-testing in this study only simulates the long-only transaction by considering the practical difficulties in real stock markets and follows the suggestion of Avramov et al. [21]. Specifically, real stock markets have restrictions for the sell-side positions, for example, the availability of the stocks for selling, variable borrowing rates for individual stocks as well as liquidity of the stock. Two simple asset allocation methods are applied for portfolio-wise back testing, which are equal-weighted and value-weighted. Equal-weighted portfolio distributes weights to 420 stocks evenly, while the value-weighted portfolio allocates the weights to stocks based on the size of the stocks' market capitalization. In this sense, in a value-weighted portfolio, stocks with larger market capitalization would be distributed with heavier weights, and the summation of all weights for these 420 stocks is equal to one. Thus, the computation of indicators in the value-weighted portfolio concentrates more on larger market

capitalization stocks.

Table 4 presents the back testing results of the equal-weighted portfolio of each model in the three periods. All models in all periods consistently outperform the buy-and-hold (BHE) strategy except for the vanilla RNN model and RNN Luong’s concatenate attention model (LC). The proposed models have the highest annulized returns during all periods. When considering the standard deviation risks (Sharpe Ratio) and downside risks (Sortino Ratio) of the returns, the proposed models achieve first place (RNN global self-attention model) and second place (RNN sliding window attention model) in Period 1911 and Period 2212. However, in Period 2112, the vanilla RNN model shows a marginal advantage on the Sharpe ratio and the Sortino ratio. The Sharpe ratio of the vanilla RNN model lies between the RNN global self-attention model (self\_att) and the RNN sliding window attention model (sparse\_att), while the Sortino ratio is higher than both proposed models. This demonstrates that the vanilla RNN model has a higher risk protection capability, especially downside risks, when it faces extreme market conditions such as a volatile market with a significant trend. GRU and LSTM models perform quite similarly in all periods. For the rest of the RNN attention models, including the RNN additive model (Batt) and the RNN Luong’s attention models (LC, LD, LG), their performance varies concerning the market conditions. In Period 1911, Model Batt is superior to Model LC, LD, LG, as well as GRU and LSTM models, and becomes the most profitable RNN attention model following the proposed models. However, when considering volatility risks, including standard deviation and downside risks, it falls behind the RNN Luong’s dot product attention model (LD). The performance of Model Batt in Period 2112 and Period 2212 is not as well as in Period 1911 when comparing with alternative RNN attention benchmark models (LC, LD, LG) and RNN variation models (GRU, LSTM) in the same period. It falls behind the LD model but still outperforms RNN variation models in both periods. For RNN Luong’s three attention models (LC, LD, LG), LD performs best in all periods which is followed by LG. These phenomena imply that all RNN attention models, apart from the LC model, are superior to the RNN variation models, especially when encountering extreme market conditions. Nonetheless, the vanilla RNN model shows a great capability to control downside risks during the market turbulence, but sacrifices its absolute returns.

Figure 13 is the diagram for the comparison of the annulized Sharpe ratio and Sortino ratio in the equal-weighted portfolios. The upper panel shows the Sharpe ratio, and the lower panel shows the Sortino ratio. It is apparent that the Sharpe ratio of the self\_att model achieves the highest value in the pre-pandemic period (1911) and the pandemic period (2112) whereas during the period that covers one year after the pandemic (2212), which contains a rapid drop and a highly fluctuating sideways movement of the price shows in Figure E5, the proposed sparse\_att wins the first place. It is also worth noting that the LD model follows closely to the performance of the proposed models and achieves third place. That implies that the attention mechanisms based dot product, including LD, self\_att and sparse\_att, demonstrate superior performance compared to other attention variants. The diagram of the Sortino ratios



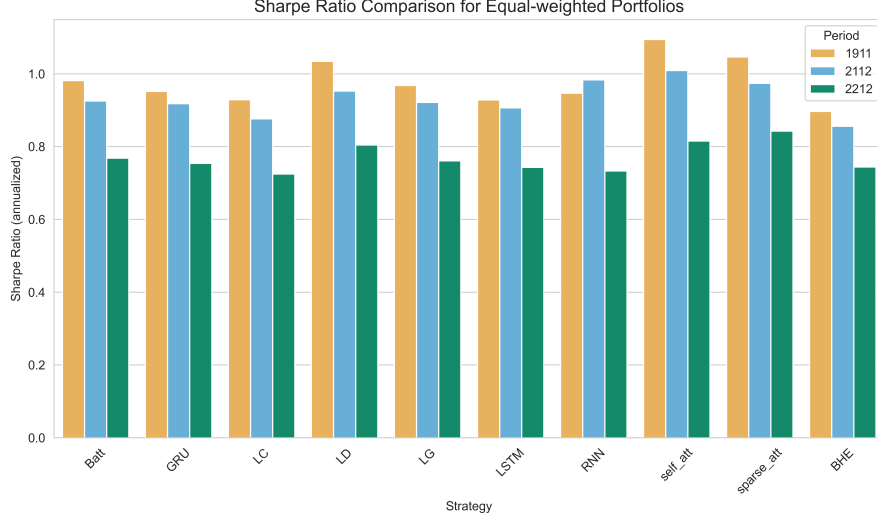
Strategy	Max Draw- down	Ann Return	Sharpe Ratio (SR)	Sortino Ratio (SO)	Returns Std	Ann SR	Ann SO
<b>1911</b>							
Batt	(0.3128)	0.1229	0.2834	0.3993	0.0353	0.9816	1.3832
GRU	(0.3241)	0.1162	0.2748	0.3853	0.0344	0.9520	1.3349
LC	(0.3564)	0.1168	0.2681	0.3760	0.0356	0.9288	1.3024
LD	(0.3077)	0.1289	0.2986	0.4259	0.0350	1.0343	1.4754
LG	(0.3180)	0.1212	0.2795	0.3954	0.0353	0.9681	1.3698
LSTM	(0.3562)	0.1166	0.2680	0.3798	0.0355	0.9283	1.3155
RNN	(0.2588)	0.1041	0.2733	0.3650	0.0308	0.9466	1.2643
self_att	(0.3008)	0.1357	0.3159	0.4570	0.0347	1.0944	1.5832
sparse_att	(0.3154)	0.1298	0.3020	0.4298	0.0348	1.0462	1.4889
BHE	(0.3701)	0.1139	0.2588	0.3631	0.0356	0.8965	1.2578
<b>2112</b>							
Batt	(0.4953)	0.1459	0.2672	0.3323	0.0453	0.9255	1.1512
GRU	(0.4932)	0.1392	0.2650	0.3279	0.0435	0.9180	1.1357
LC	(0.5212)	0.1367	0.2530	0.3100	0.0451	0.8765	1.0739
LD	(0.4820)	0.1471	0.2751	0.3370	0.0441	0.9530	1.1675
LG	(0.4886)	0.1423	0.2660	0.3317	0.0443	0.9215	1.1489
LSTM	(0.4895)	0.1395	0.2617	0.3287	0.0442	0.9067	1.1385
RNN	(0.4123)	0.1300	0.2838	0.3862	0.0372	0.9833	1.3379
self_att	(0.4427)	0.1540	0.2913	0.3823	0.0433	1.0091	1.3242
sparse_att	(0.4584)	0.1503	0.2811	0.3598	0.0440	0.9739	1.2463
BHE	(0.5310)	0.1349	0.2472	0.2988	0.0452	0.8563	1.0351
<b>2212</b>							
Batt	(0.4960)	0.1241	0.2218	0.2911	0.0476	0.7684	1.0083
GRU	(0.4968)	0.1177	0.2177	0.2835	0.0459	0.7541	0.9820
LC	(0.5208)	0.1165	0.2092	0.2707	0.0477	0.7248	0.9377
LD	(0.4731)	0.1279	0.2323	0.3021	0.0465	0.8046	1.0465
LG	(0.4933)	0.1215	0.2197	0.2875	0.0470	0.7609	0.9961
LSTM	(0.4980)	0.1181	0.2145	0.2812	0.0469	0.7430	0.9742
RNN	(0.4191)	0.1012	0.2117	0.2896	0.0400	0.7334	1.0033
self_att	(0.4409)	0.1334	0.2433	0.3336	0.0459	0.8429	1.1558
sparse_att	(0.4545)	0.1304	0.2354	0.3178	0.0467	0.8154	1.1010
BHE	(0.5308)	0.1141	0.2148	0.2760	0.048	0.7441	0.9561

**Table 4:** Equal-weighted portfolio performance. 'Ann' is the notation for annulization, while 'SR' and 'SO' are short for Sharpe ratio and Sortino ratio respectively. The notation of 'Std' means standard deviation, and 'BHV' means buy-and-hold strategy in value-weighted portfolios. The values in the parentheses indicate negative values. 'Ann Return' and 'Max Drawdown' can be transformed to a percentage presentation by multiplying by 100.

enlarges the difference between models. It supports the conclusion drawn from the diagram of the Sharpe ratios in Period 1911 and Period 2212. However, in Period 2112, the vanilla RNN model achieves the highest value with an insignificant advantage compared to the proposed models, especially the self\_att model, which implies that the vanilla RNN model has a great capability to hedge the downside risks during the extreme market fluctuations.

The equal-weighted portfolio cumulative return plot, Figure 14, agrees with the findings from Table 4. In Period 1911, the cumulative returns of the LD model and RNN sliding window attention model (sparse\_att) are similar, and the LD model outperforms the sparse\_att model in a short period, from late 2015 to the middle of 2018. However, from 2019, the proposed RNN global self-attention model shows a non-negligible advantage over alternatives, which is closely followed by the proposed RNN sliding window attention model. All models' cumulative returns outperform the buy-and-hold benchmark (BHE) and the vanilla RNN model since 2017. Apart from the LC model, all attention models show superiority to those models without attention mechanisms during the market shock periods. Model LD, Batt, LG rank in third, fourth and fifth place, respectively. Although the vanilla RNN model exhibits a great OOS fitness and ability for controlling downside risks, it sacrifices its absolute capital gain during the market fluctuations. In this respect, the vanilla RNN model is possibly more suitable for the funds that require high-capability hedging against downside risks instead of pursuing high absolute capital gain, or for modelling the market volatility.

In the value-weighted portfolios, which are shown in Table 5, apart from the proposed models and the vanilla RNN model, the annualized returns of all models in all periods are significantly higher than those in the equal-weighted portfolio. Annualized returns of the vanilla RNN model in all periods are considerably lower than those in the equal-weighted portfolio, but annualized returns of the proposed models vary according to the periods. In Period 1911 and Period 2212, the RNN global self-attention (self\_att) model's annualized return is lower than the one in the same period of the equal-weighted portfolio, and the RNN sliding window attention model's annualized return is higher than the one in the same period of the equal-weighted portfolio. However, in Period 2112, the annualized returns of the proposed models become lower than those in equal-weighted portfolios. Specifically, the difference of the annualized return in the RNN sliding window attention model (sparse\_att) is quite insignificant, but the one in self\_att is significant. Nevertheless, when returns are assessed in light of volatility risks, which are shown as the Sharpe ratio and the Sortino ratio, all models in all periods illustrate significant advantages compared with those in equal-weighted portfolios. This phenomenon implies that all models work better on stocks with larger market capitalization when considering risks, but the annualized returns variation also indicates that the vanilla RNN model and self\_att model are less preferred by larger market-cap stocks.



(a) Annualized Sharpe ratio comparison



(b) Annualized Sortino ratio comparison

**Fig. 13:** Annualized Sharpe ratio and Sortino ratio for Equal-weighted.

The rest of the findings from equal-weighted portfolios still stand for the value-weighted portfolios. All models in all periods outperform the buy-and-hold (BHV) strategy in value-weighted portfolios, excluding the vanilla RNN model in Period 1911, whose Sortino ratio is lower than that of BHV. From a full angle, value-weighted portfolios have a higher capability to moderate market fluctuation risks, and most of the

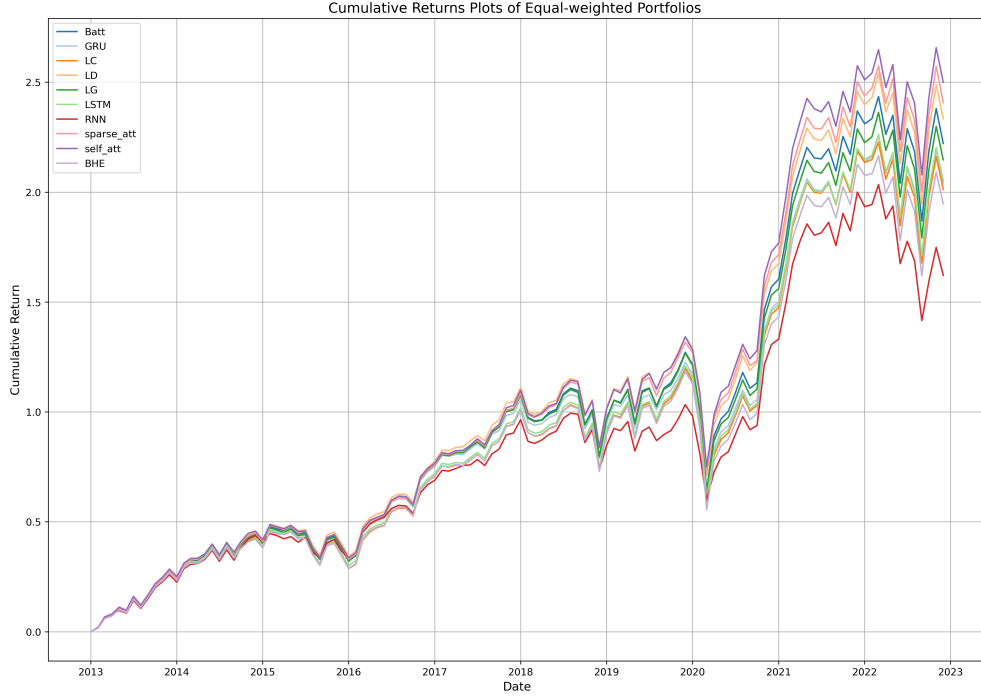


**Fig. 14:** Cumulative return plot for Equal-weighted portfolios.

models have higher annualized returns than equal-weighted portfolios. It is noteworthy to notice the rank change of the GRU model in Period 2112 of the value-weighted portfolio according to its Sortino ratio, it outperforms the RNN benchmark attention models (Batt, LC, LD, LG), demonstrating that the GRU model works more efficiently on handling the downside risk during the market turbulence for larger-cap stocks. The value-weighted portfolio cumulative return plots in Figure 16 support the conclusions drawn from Table 5.

The comparison of the Sharpe ratios and the Sortino ratios for value-weighted portfolios is exhibited in Figure 15. The value-weighted method narrows the difference in periodic performance between models. In the diagram of the Sharpe ratio, the findings are consistent with those in the diagram of the equal-weighted method. The self\_att model outperforms all alternatives, followed by the sparse\_att model. And the difference between the proposed models is negligible. All models perform similarly in Period 1911 and Period 2112, which indicates less advantage shows up for these models on larger-cap stocks when the market has a mild or sharp uptrend. However, the Sharpe ratios are significantly reduced when the market slumps. This phenomenon is less significant in the equal-weighted method. This provides indirect evidence that these models exhibit stronger effectiveness in moderating downside risks for volatile (smaller-cap) stocks. The information from the diagrams of the Sortino ratios in both portfolio weighting methods agrees with this stand. However, the noticeably

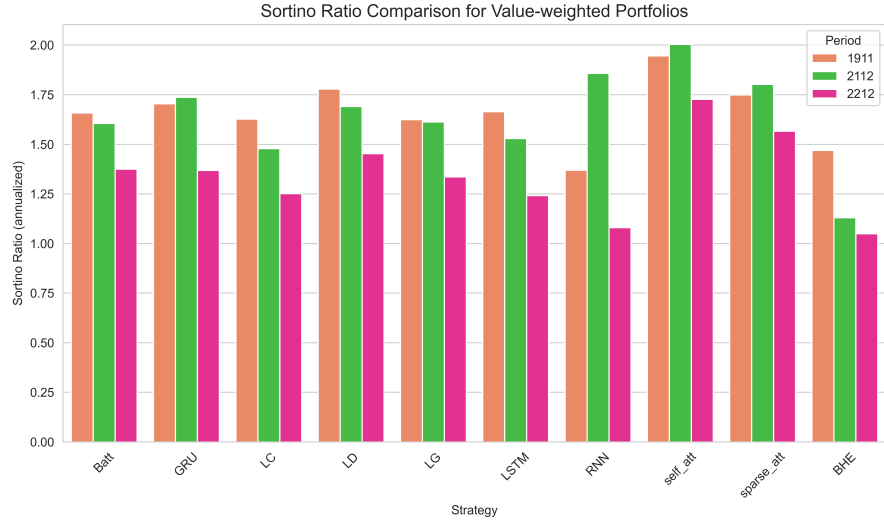
Strategy	Max Draw-down	Ann Return	Sharpe Ratio (SR)	Sortino Ratio (SO)	Returns Std	Ann SR	Ann SO
<b>1911</b>							
Batt	(0.2526)	0.1338	0.3507	0.4787	0.0300	1.2149	1.6582
GRU	(0.2494)	0.1335	0.3578	0.4922	0.0293	1.2394	1.7049
LC	(0.2639)	0.1319	0.3400	0.4699	0.0306	1.1777	1.6278
LD	(0.2196)	0.1343	0.3634	0.5135	0.0290	1.2589	1.7787
LG	(0.2460)	0.1302	0.3499	0.4692	0.0292	1.2122	1.6252
LSTM	(0.2477)	0.1363	0.3496	0.4806	0.0307	1.2112	1.6649
RNN	(0.2848)	0.0827	0.3021	0.3955	0.0212	1.0466	1.3701
self_att	(0.2560)	0.1299	0.3800	0.5616	0.0267	1.3164	1.9455
sparse_att	(0.2258)	0.1339	0.3713	0.5048	0.0282	1.2864	1.7488
BHV	(0.2963)	0.1197	0.2956	0.4243	0.0323	1.0240	1.4698
<b>2112</b>							
Batt	(0.3034)	0.1515	0.3383	0.4636	0.0355	1.1720	1.6060
GRU	(0.2684)	0.1474	0.3488	0.5016	0.0333	1.2083	1.7377
LC	(0.3394)	0.1487	0.3224	0.4270	0.0367	1.1167	1.4792
LD	(0.2888)	0.1524	0.3511	0.4881	0.0343	1.2161	1.6907
LG	(0.2895)	0.1473	0.3446	0.4656	0.0338	1.1936	1.6129
LSTM	(0.3264)	0.1539	0.3322	0.4414	0.0368	1.1509	1.5292
RNN	(0.2811)	0.1071	0.3497	0.5364	0.0238	1.2112	1.8581
self_att	(0.2829)	0.1395	0.3706	0.5785	0.0295	1.2837	2.0039
sparse_att	(0.2483)	0.1498	0.3677	0.5204	0.0320	1.2737	1.8028
BHV	(0.4513)	0.1337	0.2673	0.3263	0.0408	0.9260	1.1303
<b>2212</b>							
Batt	(0.2996)	0.1297	0.2757	0.3970	0.0380	0.9551	1.3754
GRU	(0.2915)	0.1241	0.2745	0.3952	0.0364	0.9507	1.3690
LC	(0.3354)	0.1271	0.2599	0.3615	0.0398	0.9003	1.2524
LD	(0.2691)	0.1308	0.2883	0.4195	0.0364	0.9985	1.4533
LG	(0.2989)	0.1268	0.2742	0.3858	0.0373	0.9500	1.3366
LSTM	(0.3410)	0.1301	0.2623	0.3585	0.0404	0.9087	1.2420
RNN	(0.3113)	0.0773	0.2295	0.3120	0.0266	0.7951	1.0807
self_att	(0.2581)	0.1240	0.3120	0.4985	0.0315	1.0808	1.7269
sparse_att	(0.2462)	0.1354	0.3070	0.4523	0.0351	1.0636	1.5668
BHV	(0.4513)	0.1156	0.2311	0.3031	0.0438	0.8006	1.0500

**Table 5:** Value-weighted portfolio performance. 'Ann' is the notation for annulization, while 'SR' and 'SO' are short for Sharpe ratio and Sortino ratio respectively. The notation of 'Std' means standard deviation, and 'BHE' means buy-and-hold strategy in equal-weighted portfolios. The values in the parentheses indicate negative values. 'Ann Return' and 'Max Drawdown' can be transformed to a percentage presentation by multiplying by 100.

high sortino ratio of the vanilla RNN model in Period 2112 reflects the sensitivity of the vanilla RNN model towards the downside risks caused by the extreme market turbulence when larger market capitalization presents. Model GRU shows similar characteristics.



(a) Annualized Sharpe ratio comparison



(b) Annualized Sortino ratio comparison

**Fig. 15:** Annualized Sharpe ratio and Sortino ratio for Value-weighted.

From the cumulative return plot Figure 16 in the value-weighted method, we can see value-weighted portfolios narrow the difference between models to a degree during the pandemic and post-pandemic period, except for the vanilla RNN model, self\_att model and buy-and-hold (BHV) benchmark. The performance of the proposed

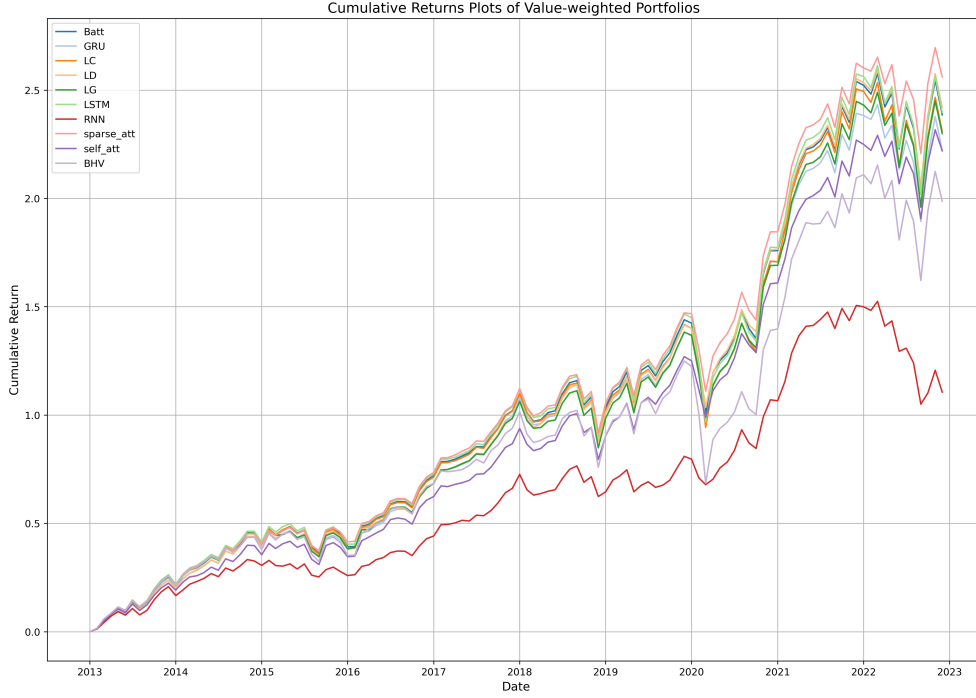


**Fig. 16:** Cumulative return plot for Value-weighted portfolios.

sparse\_att model is stable in both the equal-weighted portfolios and the value-weighted portfolios, and it ranks as the best model after 2016 due to the best model in the equal-weighted portfolios, self\_att, dropping behind all RNN attention benchmark models and RNN variation models and losing its advantage when heavy weights are added to the larger-cap stocks. This phenomenon implies that the self\_att model latently performs better on smaller-cap stocks, and it is sensitive to variations in time series. The variation is larger, the performance of the self\_att is better. A similar phenomenon happens on the GRU model as well, while it drops right before the rank of the self\_att model during the market turbulence in the value-weighted case. However, the other RNN variation model, LSTM, presents a great capability in profitability among the larger-cap stocks, which ranks in first place before 2016 and second place after 2016. Likewise, the LD model remains the third place in the value-weighted case, which means Model sparse\_att and Model LD are less likely to be affected by the size of stocks' market capitalization. They consistently possess great back-testing performance, which implies they are suitable for stocks with different levels of volatility. It is also interesting to notice that the vanilla RNN model performs worse in cumulative return plots. It shows the capacity for hedging downside risks instead of deriving the absolute returns, but it does not work well during market turbulence when heavy weights are given to larger-cap stocks. It indicates a preference for volatile stocks.

## 6 Conclusion

This study investigates the pretrained RNN attention models with the mainstream attention mechanisms such as additive attention [30], Luong’s three attentions [31], global self-attention [11] and sliding window sparse attention [12] for the empirical asset pricing assignment. The research emphasises the pretrained RNN global self-attention model (self\_att) and the pretrained RNN sliding window sparse attention model (sparse\_att) as they are the innovative structures in different domains, especially for NLP. Less literature systematically investigates the role of attention mechanisms in the context of asset pricing. This is the first empirical asset pricing research which employs the RNN frames with the global self-attention mechanism, sliding window sparse attention mechanism and Luong’s three attention mechanisms [31]. They solve or moderate the issues in classic ML model-based empirical asset pricing research, such as sequence or time-series data recognition, models’ financial or economic interpretability and overfitting caused by over-parameterization of the ML models. It also investigates the necessity of the attention mechanisms in the context of ML-based asset pricing by constructing the benchmark models of the pre-trained RNN additive attention model (Batt), Luong’s three attention models (LG, LD, LC) and no-attention RNN models (RNN, LSTM, GRU). Moreover, all models are evaluated and portfolio-wise backtested in three periods: pre-COVID-19 (1911), COVID-19 (2112), and one year post-COVID-19 (2212) - to prove whether the model has the capability to handle extreme market conditions. These capabilities include absolute and risk-considered profitability during extreme market turbulence. In summary, this study pursues two objectives across two dimensions: 1) to examine whether the factors in the proposed and alternative structures can better explain the stock excess returns and satisfy the no-arbitrage assumption in the background of ‘factor zoo’, which is one direction of empirical asset pricing research. 2) to examine the predictability and trading strategy-wise profitability of these models, which is the goal of the factor investing studies for practitioners.

The results from model performance evaluation find that the vanilla RNN model has the highest model out-of-sample fitness, followed by Model self\_att and Model sparse\_att, during all periods. The proposed models present stability during the extreme market fluctuations, especially for the sparse\_att model. This confirms the predictability of the vanilla RNN model and the proposed models to some extent. The average positive values of residual  $\alpha$  and distribution plots of  $\alpha$  provide strong evidence for the existence of market arbitrage opportunities during the three periods. These are anomalies caused by mispricing in empirical asset pricing literature, and it is where factor investors can benefit from. The significant increase in the average  $\alpha$  of all models in Period 2112, which follows the trend of the price index, along with the modest differences between models within each period, further reduces the likelihood of model misspecification. This study successfully explores the meaning of the residual  $\alpha$  in ML-based asset pricing.



From portfolio-wise back testing, the `self_att` model outperforms all alternative models when returns are considered in conjunction with risks in both equal-weighted portfolios and value-weighted portfolios, followed by the `sparse_att` model. However, when returns are not considered with risks, Model `self_att` is the best in equal-weighted portfolios, but deteriorates in value-weighted portfolios. Instead, Model `sparse_att` shows some stability, which is in the second place of equal-weighted portfolios but is the best in the value-weighted portfolios. This implies that the `self_att` model performs better on smaller market-cap stocks. This verifies the conclusions from the self-attention literature, which includes the classic Transformer literature, that the self-attention mechanism has higher sensitivity to the large variation between time steps, which makes it capable of modelling the highly volatile data. On the other hand, the `sparse_att` model is not affected by the stock market capitalisation. It stably provides excellent performance without considering the volatility of the stocks. Namely, it is more generalized than the `self_att` model, which is great news for both practitioners and academic scholars. Additionally, the benchmark RNN attention models in equal-weighted portfolios generally equal or outperform the models without an attention mechanism, apart from the RNN Luong’s concatenate attention model (LC). Nevertheless, it varies in value-weighted portfolios. The market capitalization weights seem to significantly reduce the benefit of attention mechanisms if we only consider the absolute returns. Moreover, value-weighted portfolios narrow the difference between models. Thus, the advantage of the attention mechanism is not as significant as in the equal-weighted portfolios. The overall performance of value-weighted portfolios is higher than equal-weighted portfolios. Approximately, all models somehow show the capability of handling the downside risks during the period with pandemic effect, while all models outperform the buy-and-hold strategy in both portfolio groups, excluding the vanilla RNN model. And it is also interesting to notice that this model fails in the back-testing model competition, especially on the absolute returns of value-weighted portfolios. This indicates that it is easily affected by the stock volatility level. From the perspective of the Sharpe ratios, this work supports the findings from Chatigny et al. [29] that in value-weighted portfolios, the large-cap stocks achieve the annualized Sharpe ratio above 1.0, but it does not persist during the period that the market was experiencing the sideways movement with extreme fluctuations.

This study also finds some interesting research questions for further discussion. Although this work covers large-scale factors, these factors are pre-selected, which indicates that the issue of omitted factors may exist. The positive  $\alpha$  values also imply this issue. Thus, alternative methods can be proposed as a substitute for the pre-selecting factors. Moreover, literature on ML-based asset pricing neglects the discussion on how to decide the number of abstracted or transformed factors. It is worth exploring the method for determining factor numbers via the ML approaches. Furthermore, it could be interesting to explore the structure of  $\alpha$ s and how to interpret these  $\alpha$ s in the ML-based asset pricing research. Finally, this study only adopts the simple asset allocation strategies, equal-weighted and value-weighted, but intuitively, ML methods can be deployed for asset allocation to further improve the strategic

returns of portfolios.

To conclude, 'attention' is something worth exploring further, but far from 'all we need' in the context of the empirical asset pricing.

**Acknowledgements.** I would like to express my sincere gratitude to my supervisor, Professor Peter N. Smith (University of York), for his patient guidance, constant encouragement, and invaluable support throughout this project. I am also grateful to Dr Jiaying Peng (University of York) for the advice on the data source. This research was supported by the Viking Computing Centre (University of York) through access to its GPU-based high-performance computing (HPC) cluster.

Constructive feedback is greatly appreciated.

## References

- [1] Lai, S.: Multilayer perceptron neural network models in asset pricing: An empirical study on large-cap us stocks. arXiv preprint arXiv:2505.01921 (2025)
- [2] Harvey, C.R., Liu, Y., Zhu, H.: ... and the Cross-Section of Expected Returns. *Review of Financial Studies* **29**(1), 5–68 (2016) <https://doi.org/10.1093/rfs/hhv059>
- [3] Gu, S., Kelly, B., Xiu, D.: Empirical Asset Pricing via Machine Learning. *Review of Financial Studies* **33**(5), 2223–2273 (2020) <https://doi.org/10.1093/rfs/hhaa009>
- [4] Coqueret, G., Guida, T.: *Machine Learning for Factor Investing: R Version*. CRC Press, Boca Raton, FL (2020)
- [5] Andrew Y.; Zimmermann, T.C.: Open source cross-sectional asset pricing. Centre for Financial Research (CFR), working paper (2020)
- [6] Zhou, X., Wang, Y.: Learning from memory: Asset pricing via recurrent neural network and attention mechanism. Available at SSRN 4999011 (2024)
- [7] Elman, J.L.: Finding structure in time. *Cognitive science* **14**(2), 179–211 (1990)
- [8] Rumelhart, D.E., Hinton, G.E., Williams, R.J.: Learning representations by back-propagating errors. *nature* **323**(6088), 533–536 (1986)
- [9] Hochreiter, S., Schmidhuber, J.: Long short-term memory. *Neural computation* **9**(8), 1735–1780 (1997)
- [10] Cho, K., Merriënboer, B.V., Gulcehre, C., Bahdanau, D., Bougares, F., Schwenk, H., Bengio, Y.: Learning phrase representations using RNN encoder-decoder for statistical machine translation. In: *EMNLP 2014 - 2014 Conference on Empirical Methods in Natural Language Processing, Proceedings of the Conference*, pp. 1724–1734 (2014). <https://doi.org/10.3115/v1/d14-1179>
- [11] Vaswani, A., Shazeer, N., Parmar, N., Uszkoreit, J., Jones, L., Gomez, A.N., Kaiser, Ł., Polosukhin, I.: Attention is all you need. *Advances in neural information processing systems* **30** (2017)
- [12] Beltagy, I., Peters, M.E., Cohan, A.: Longformer: The long-document transformer. arXiv preprint arXiv:2004.05150 (2020)
- [13] Kelly, B.T., Kuznetsov, B., Malamud, S., Xu, T.A.: Artificial intelligence asset pricing models. Technical report, National Bureau of Economic Research (2025)
- [14] Fama, E.F., French, K.R.: Common risk factors in the returns on stocks and bonds. *Journal of Financial Economics* **33**(1), 3–56 (1993) [https://doi.org/10.1016/0304-3865\(93\)90026-2](https://doi.org/10.1016/0304-3865(93)90026-2)

- [15] Carhart, M.M.: On persistence in mutual fund performance. *Journal of Finance* **52**(1), 57–82 (1997) <https://doi.org/10.1111/j.1540-6261.1997.tb03808.x>
- [16] Fama, E.F., French, K.R.: A five-factor asset pricing model. *Journal of Financial Economics* **116**(1), 1–22 (2015) <https://doi.org/10.1016/j.jfineco.2014.10.010>
- [17] Hou, K., Xue, C., Zhang, L.: Digesting anomalies: An investment approach. *Review of Financial Studies* **28**(3), 650–705 (2015) <https://doi.org/10.1093/rfs/hhu068>
- [18] Harvey, C.R., Liu, Y.: A census of the factor zoo. Available at SSRN 3341728 (2019)
- [19] Wang, Q.: Cryptocurrencies asset pricing via machine learning. *International Journal of Data Science and Analytics* **12**(2), 175–183 (2021) <https://doi.org/10.1007/s41060-021-00252-6>
- [20] Gu, S., Kelly, B., Xiu, D.: Autoencoder asset pricing models. *Journal of Econometrics* **222**(1), 429–450 (2021)
- [21] Avramov, D., Cheng, S., Metzker, L.: Machine learning versus economic restrictions: Evidence from stock return predictability. Available at SSRN 3450322 (2021)
- [22] Chen, L., Pelger, M., Zhu, J.: Deep Learning in Asset Pricing. *Management Science* **70**(2), 714–750 (2024) <https://doi.org/10.1287/mnsc.2023.4695>
- [23] Kelly, B.T., Pruitt, S., Su, Y.: Characteristics are covariances: A unified model of risk and return. *Journal of Financial Economics* **134**(3), 501–524 (2019) <https://doi.org/10.1016/j.jfineco.2019.05.001>
- [24] Bagnara, M.: Asset Pricing and Machine Learning: A critical review. *Journal of Economic Surveys* (2022) <https://doi.org/10.1111/joes.12532>
- [25] Goodfellow, I.J., Pouget-Abadie, J., Mirza, M., Xu, B., Warde-Farley, D., Ozair, S., Courville, A., Bengio, Y.: Generative adversarial nets. *Advances in neural information processing systems* **27** (2014)
- [26] Ma, T., Wang, W., Chen, Y.: Attention is all you need: An interpretable transformer-based asset allocation approach. *International Review of Financial Analysis* **90** (2023) <https://doi.org/10.1016/j.irfa.2023.102876>
- [27] Zhang, C.: Asset pricing and deep learning. arXiv preprint arXiv:2209.12014 (2022)

- [28] Cong, L.W., Tang, K., Wang, J., Zhang, Y.: Deep sequence modeling: Development and applications in asset pricing. arXiv preprint arXiv:2108.08999 (2021)
- [29] Chatigny, P., Goyenko, R., Zhang, C.: Asset pricing with attention guided deep learning. Available at SSRN 3971876 (2021)
- [30] Bahdanau, D., Cho, K.H., Bengio, Y.: Neural machine translation by jointly learning to align and translate. In: 3rd International Conference on Learning Representations, ICLR 2015 - Conference Track Proceedings, pp. 1–15 (2015)
- [31] Luong, M.-T., Pham, H., Manning, C.D.: Effective approaches to attention-based neural machine translation. arXiv preprint arXiv:1508.04025 (2015)
- [32] Akhtar, M.S., Kumar, A., Ghosal, D., Ekbal, A., Bhattacharyya, P.: A multilayer perceptron based ensemble technique for fine-grained financial sentiment analysis. In: Proceedings of the 2017 Conference on Empirical Methods in Natural Language Processing, pp. 540–546 (2017)
- [33] Sagiraju, H.K., Mogalla, S.: Application of multilayer perceptron to deep reinforcement learning for stock market trading and analysis. Indonesian Journal of Electrical Engineering and Computer Science **24**(3), 1759–1771 (2021)
- [34] Bao, W., Yue, J., Rao, Y.: A deep learning framework for financial time series using stacked autoencoders and long-short term memory. PloS one **12**(7), 0180944 (2017)
- [35] Bieganski, B., Slepaczuk, R.: Supervised autoencoder mlp for financial time series forecasting. arXiv preprint arXiv:2404.01866 (2024)
- [36] Heaton, J.B., Polson, N.G., Witte, J.H.: Deep learning for finance: deep portfolios. Applied Stochastic Models in Business and Industry **33**(1), 3–12 (2017)
- [37] Bengio, Y., Simard, P., Frasconi, P.: Learning long-term dependencies with gradient descent is difficult. IEEE transactions on neural networks **5**(2), 157–166 (1994)
- [38] Gers, F.A., Schmidhuber, J., Cummins, F.: Learning to forget: Continual prediction with lstm. Neural computation **12**(10), 2451–2471 (2000)
- [39] Jozefowicz, R., Zaremba, W., Sutskever, I.: An empirical exploration of recurrent network architectures. In: International Conference on Machine Learning, pp. 2342–2350 (2015). PMLR
- [40] Galphade, M., Nikam, V., Banerjee, B., Kiwelekar, A.W.: Comparative analysis of wind power forecasting using lstm, bilstm, and gru. In: International Conference on Frontiers of Intelligent Computing: Theory and Applications, pp. 483–493

(2022). Springer

- [41] Pudikov, A., Brovko, A.: Comparison of lstm and gru recurrent neural network architectures. International Scientific and Practical Conference in Control Engineering and Decision Making, pp. 114–124 (2020). Springer
- [42] Diebold, F.X., Mariano, R.S.: Comparing predictive accuracy. Journal of Business and Economic Statistics **13**(3), 253–263 (1995)

## Appendix A Out-of-sample $\alpha$ distributions for alternative models

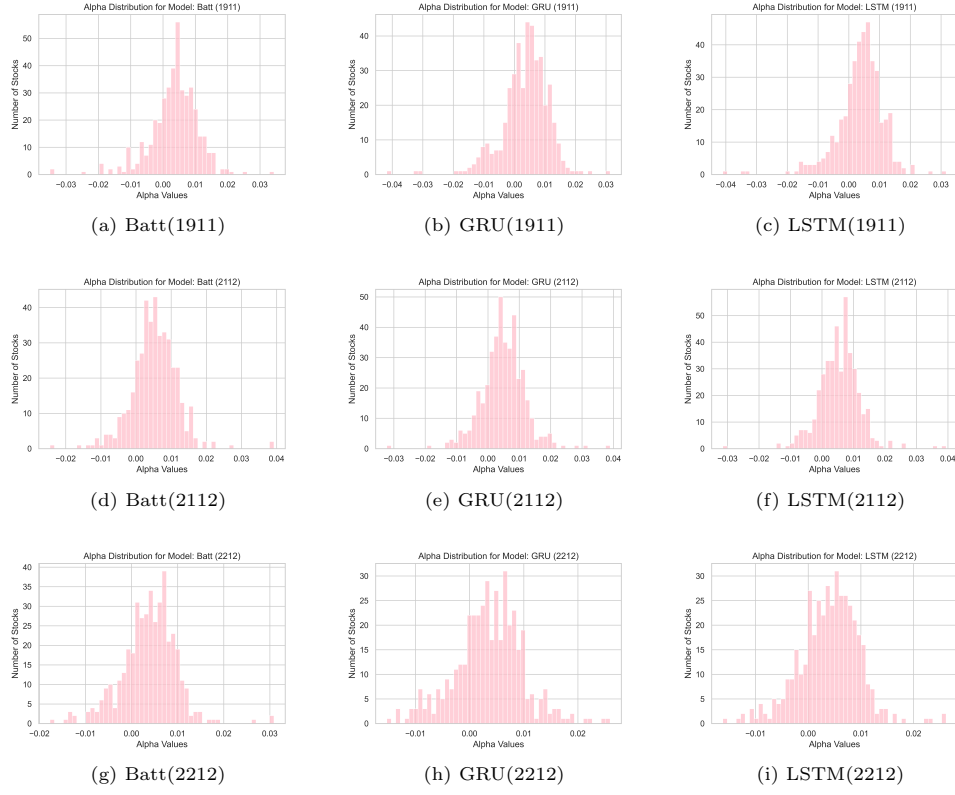


**Fig. A1:** OOS  $\alpha$  distribution of the alternative models Part 1

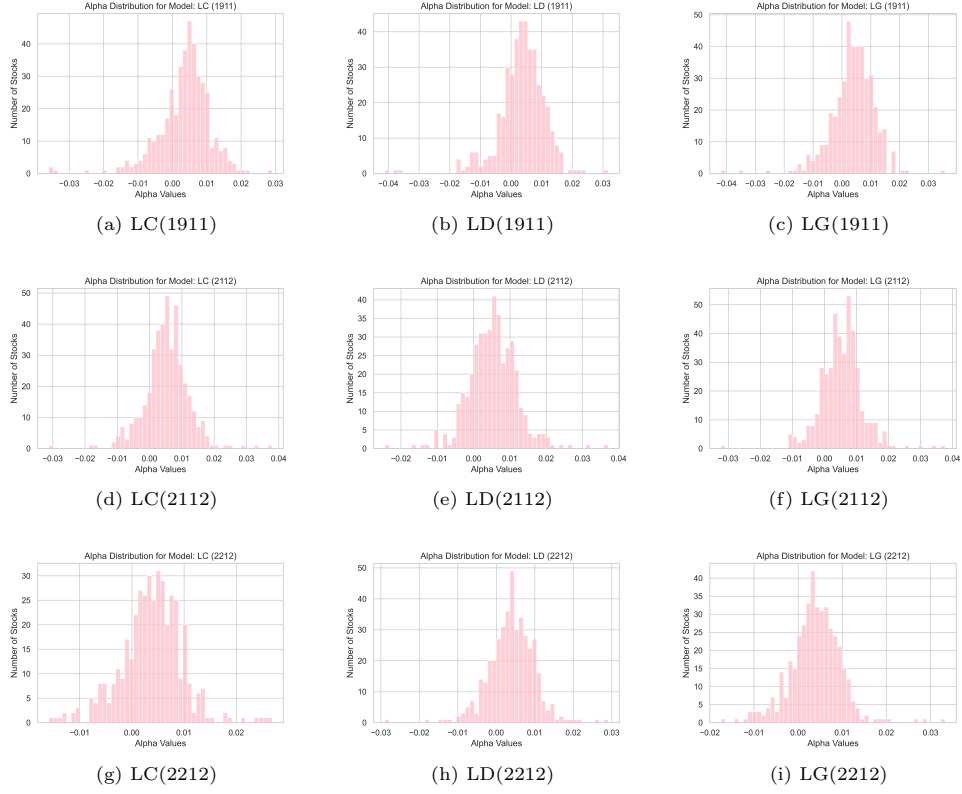


**Fig. A2:** OOS  $\alpha$  distribution of the alternative models Part 2

## Appendix B Adam optimizer

Adam updates parameters by maintaining the first and second moments of the gradients.



---

**Algorithm 1** Adam Optimization

---

```
1: Initialize:  $m_0 = 0, v_0 = 0, l = 0$ 
2: Set hyperparameters: learning rate  $\eta = 0.001, \beta_1 = 0.9, \beta_2 = 0.999, \epsilon = 10^{-8}$ 
3: while  $\theta_l$  not converged do
4:    $l \leftarrow l + 1$ 
5:   Compute gradient:  $g_l = \nabla_{\theta} L(\theta_{l-1})$ 
6:    $m_l \leftarrow \beta_1 m_{l-1} + (1 - \beta_1) g_l$ 
7:    $v_l \leftarrow \beta_2 v_{l-1} + (1 - \beta_2) g_l \odot g_l$   $\triangleright \odot$ : element-wise multiplication
8:    $\hat{m}_l \leftarrow \frac{m_l}{1 - \beta_1^l}$   $\triangleright$  Bias correction
9:    $\hat{v}_l \leftarrow \frac{v_l}{1 - \beta_2^l}$ 
10:   $\theta_l \leftarrow \theta_{l-1} - \eta \cdot \frac{\hat{m}_l}{\sqrt{\hat{v}_l} + \epsilon}$ 
11: end while
12: Return:  $\theta_l$ 
```

*Source: Adapted from Gu et al. [3]*

---

where  $g_t$  and  $\theta_t$  represent the gradients and parameters computed from previous sections respectively.

## Appendix C Early Stopping

---

**Algorithm 2** Early Stopping

---

```
1: Initialize:  $j = 0, \epsilon = \infty$ , select patience parameter  $p$ .
2: while  $j < p$  do
3:   Update  $\theta$  using the training algorithm (e.g., for  $h$  steps).
4:   Calculate the prediction error from the validation sample, denoted as  $\epsilon'$ .
5:   if  $\epsilon' < \epsilon$  then
6:      $j \leftarrow 0$ 
7:      $\epsilon \leftarrow \epsilon'$ 
8:      $\theta' \leftarrow \theta$ 
9:   else
10:     $j \leftarrow j + 1$ 
11:   end if
12: end while
13: Return:  $\theta'$ 
```

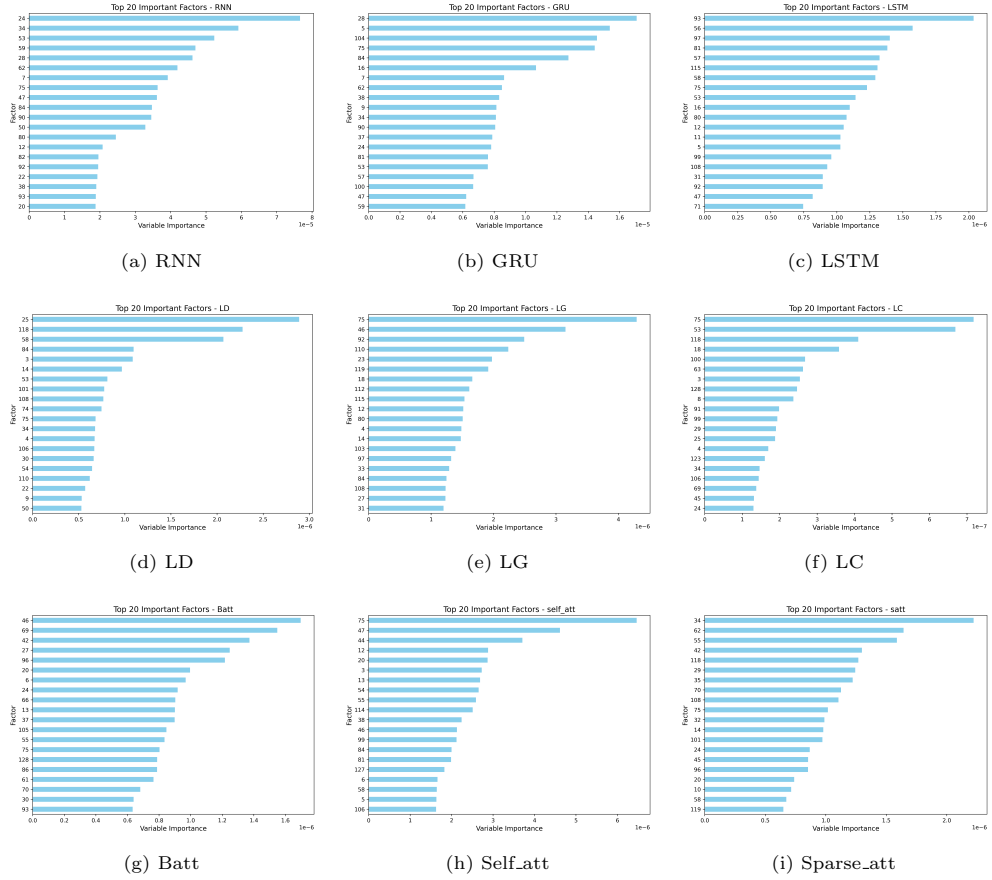
*Source: Adapted from Gu et al. [3]*

---

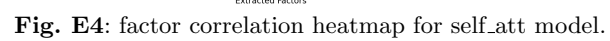
## Appendix D List of Abbreviations

RNN	pretrained vanilla recurrent neural network model
GRU	pretrained RNN with Gated Recurrent Unit
LSTM	pretrained RNN with Long Short-Term Memory
Batt	pretrained RNN additive attention model
LC	pretrained RNN Luong's concatenate attention model
LD	pretrained RNN Luong's dot product attention model
LG	pretrained RNN Luong's general attention model
self_att	pretrained RNN global self-attention model
sparse_att	pretrained RNN sliding window sparse attention model

## Appendix E Variable Importance



**Fig. E3:** Factor importance of different models



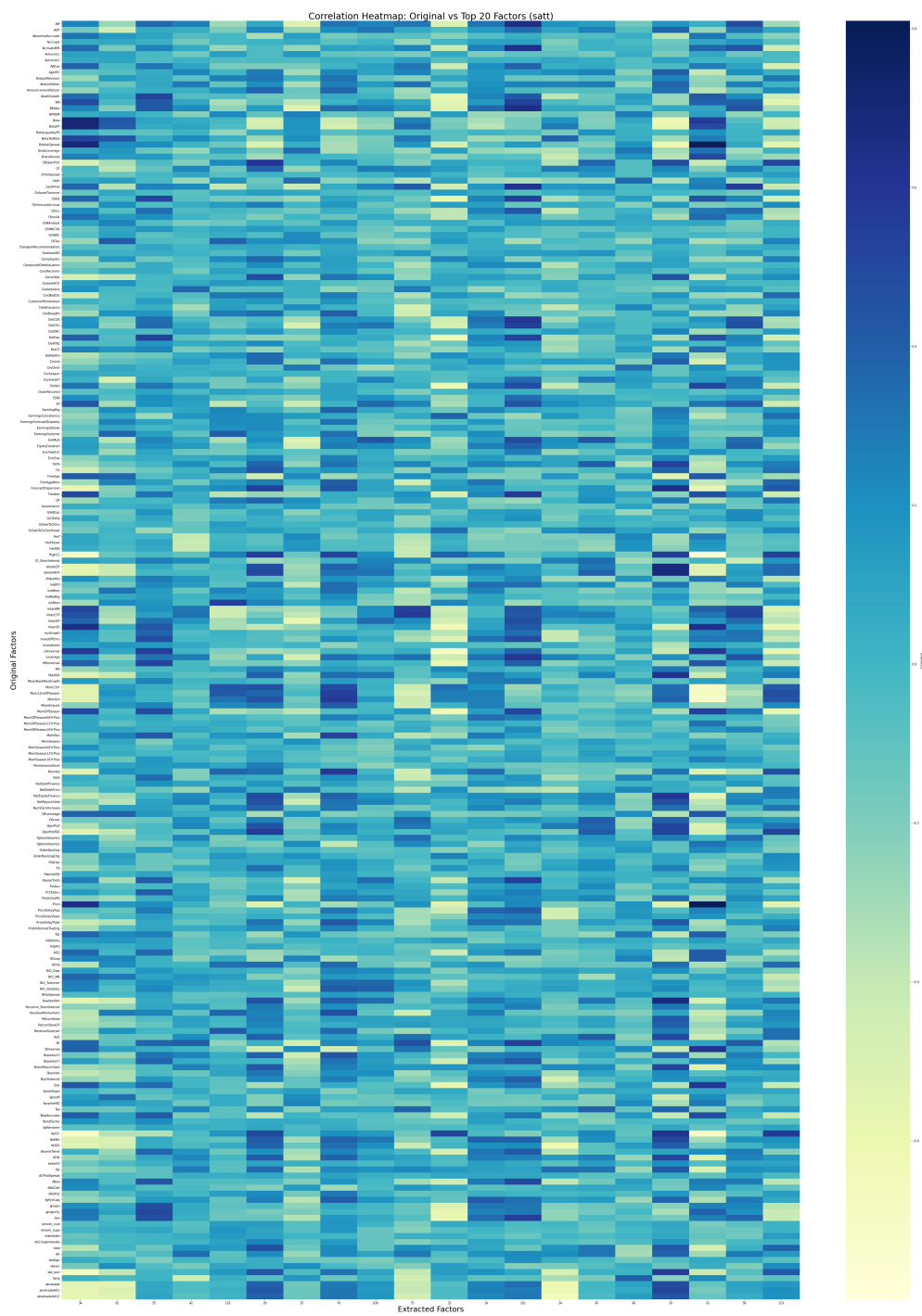


**Fig. E5:** factor correlation heatmap for sparse\_att model.